Politecnico di Torino

Department of Environment, Land and Infrastructure Engineering

Master of Science in Georesources and Geoenergy Engineering

A.Y. 2023/2024

Conversion of depleted gas reservoirs into underground CO_2 storage.

Supervisors:
Prof. Francesca VERGA
Alessandro SURIANO

Candidate:
Antonella EL KADDOUM

Abstract

One of the most important problems facing the environment nowadays is climate change. CCS (carbon capture and storage) has been considered a promising mitigation technology that can help in reaching the decarbonization goal and contribute to the climate change mitigating efforts. After presenting an overview of the CCS technology, the various storage types and the importance of the trapping mechanisms, numerical simulations and models will be investigated to understand the major effect of the reservoir and injection parameters on the injection process of CO2. A detailed sensitivity analysis was performed, investigating some key factors to determine their impact on the storage capacity as well as on the injectivity. These factors included depth and size of the reservoir, dimension of the surrounding aquifer, petrophysical properties, and injectivity parameters. The findings were compared and discussed to provide insights into the storage capacity of CO2 into various geological formations characterized by different parameters and the injectivity based on different injection strategies. The results show that the structural trapping is the dominant mechanism in all sensitivities, the mineral trapping is strongly affected by depth variation, residual trapping potential strongly regulated by the percentage of residual gas, moreover, the solubility trapping changes significantly with the irreducible water saturation as well as with the aquifer size. Permeability and porosity both play an important role in the dissipation of the pressure in the reservoir. Furthermore, injection rates have a direct correlation with the injectivity in the reservoir as well as the ramp up injection strategy offer a good control of the well-bottom hole maximum delta pressure with the increase in the ramp-up steps.

Table of Contents

List of Figures

List of tables

Scope of Work

This thesis focuses on the storage of CO_2 in underground depleted gas reservoirs to explore how various parameters affect storage capacity and injectivity. Different reservoir models representing various geological scenarios are analyzed to assess the influence of key factors on CO_2 storage. By simulating these parameters, this study aims to provide insights into their importance in CO_2 storage projects and assess how different parameters impact the feasibility and effectiveness of CO_2 storage.

The research focuses on eleven critical factors that play significant roles in CO2 storage within depleted gas reservoirs:

- **Depth**: The depth at which the reservoir is located affecting pressure and temperature conditions, influencing CO_2 behavior and storage stability.
- **Reservoir Size (GOIP)**: The size of the reservoir determines the volume available for CO_2 storage and affects the overall storage capacity.
- **Aquifer Size**: The presence and size of aquifers surrounding the reservoir and their impact on pressure management and CO_2 containment.
- **Porosity**: The percentage of pore space within the reservoir rock.
- **Anisotropy Ratio**: Describes how properties like permeability varying in different directions within the reservoir can affect the flow of CO_2.
- **Absolute Permeability**: Defines how easily fluids can flow through the reservoir rock.
- **Residual Gas Saturation**: The amount of gas remaining in the reservoir after production and its effect on the storage as well as on the fluid flow.
- **Irreducible Water Saturation**: The minimum amount of water that remains in the reservoir after production and its impact on CO_2 storage capacity and flow.
- **Maximum Gas Relative Permeability**: Describes the ability of the reservoir rock to allow CO_2 to flow relative to other fluids.
- **Injection Rate**: The rate at which CO_2 is injected into the reservoir affects pressure buildup and distribution within the formation.
- **Ramp-Up Injection Strategy**: Refers to the approach of gradually increasing CO_2 injection rates to optimize storage efficiency and mitigate operational risks.

This thesis begins with a general overview on the Carbon Storage technology highlighting different storage types and trapping mechanisms.

Afterwards, a regional characterization of the storage site is presented, detailing the geological properties and specific parameters of the reservoir models used. It includes an analysis of the production phase to establish initial conditions and understand the historical dynamics of the reservoirs.

Moving into the injection phase, the research conducts different sensitivity analyses on the pre-mentioned parameters. These analyses aim to quantify and qualify how different parameters and factors impact the storage capacity and injectivity of CO_2. By systematically varying these parameters, the study seeks to build a robust understanding of their relative importance and interactions in CO_2 storage feasibility.

At the end, a comparative analysis of results will be built across the different scenarios of CO_2 storage in depleted gas reservoirs. This comparative approach aims to highlight variations and impacts, offering valuable insights for optimizing CO_2 storage strategies and informing future geological storage projects.

I. Introduction

Climate change has become, in recent years, a central topic of discussion globally. The effects of climate change that scientists had always predicted are now occurring all over the world; ice shields are melting, sea level is rising, heat waves, global temperature rise… and its main reason is very well-known: greenhouse gas emissions.

In fact, greenhouse gases absorb heat energy and reflect it back into their surroundings and this forms the core of Earth's natural greenhouse effect. Without them, Earth's average temperature would be below freezing. However, adding extra greenhouse gases boosts this greenhouse effect causing the earth's temperature to rise, which means that too many greenhouse gases absorb the sun's energy and consequently the planet slowly warms up. Unfortunately, that's what is occurring nowadays: carbon dioxide is tipping the greenhouse effect out of balance, knowing that CO_2 is one of the most important greenhouse gases on the planet. [2 -3]

Carbon dioxide emissions are distributed in several sectors all over the world but in general the atmospheric concentrations of CO_2 are increasing mostly because of the fossil fuels that are burnt for energy purposes. Based on the IEA report, the energy sector participates in 75% of greenhouse gas production. [10] However, considering only CO_2 emissions (Fig.1), the energy sector carbon emissions reduce to 40% but it still represents the main contributing sector.

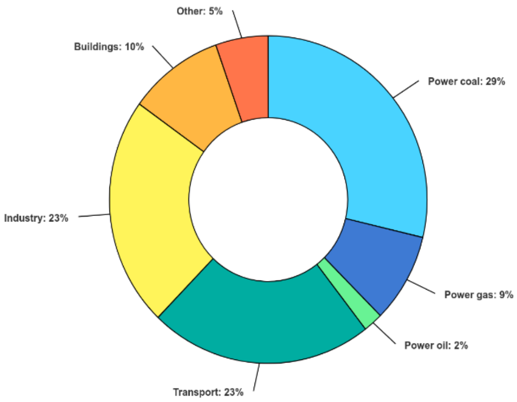

Figure 1 CO_2 emissions by sector. [4]

Nowadays, carbon dioxide levels are at the highest level ever in human history. Based on the annual report from NOAA's Global Monitoring Lab, global average atmospheric carbon dioxide was 419.3 ppm in 2023.

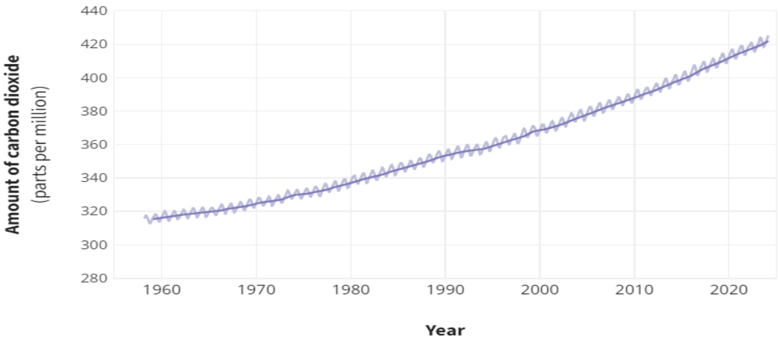

Figure 2 Graph representing amount of atmospheric CO_2.[37]

If global energy demand continues to rise fast predominantly fueled with fossil fuels, human emissions of carbon dioxide might reach 75 billion tons per year or more by the end of this century [37].

With this growing threat to our communities and future generations, governments found themselves obligated to take quick action to address this important issue that requires international cooperation and coordinated measures at all levels. Consequently, the UN Climate Change Conference (COP21) was led in Paris, France, on 12 December 2015 where the well-known “Paris Agreement” was adopted.

The Paris Agreement’s main objective is to keep "the increase in the global average temperature to well below 2°C above pre-industrial levels" and to work "to limit the temperature increase to 1.5°C above pre-industrial levels." However, in recent years, international leaders have pointed out the need to restrict global warming to 1.5°C by the end of the century. To do so, greenhouse gas emissions must peak before 2025 and fall 43% by 2030. In alignment with this agreement, various entities supported the Net Zero emission 2050 scenario that shows a pathway for the global energy sector to achieve net zero CO_2 emissions by 2050. Moreover, the European union is taking lead in combatting climate change by defining the European Green Deal that defines a strategy towards a prosperous, resource-efficient society. [7-8]

A net-zero energy system necessitates an important shift in the way we generate and consume energy, which can be accomplished through a wide range of technologies. Mitigation options may consist of the switch to renewable energy sources, energy efficiency improvements, reduction of non-CO_2 greenhouse gas emissions…

Carbon capture, utilization, and storage (CCUS) is the only group of technologies that helps directly in limiting emissions in major sectors while also removing CO_2 to balance emissions that are difficult to prevent, which is a fundamental component of "net" zero targets. [9]

Based on analysis published by IPCC, IEA and many others, it is widely clear that net-emissions targets are impossible to be achieved without CCUS alongside all other climate mitigation technologies.

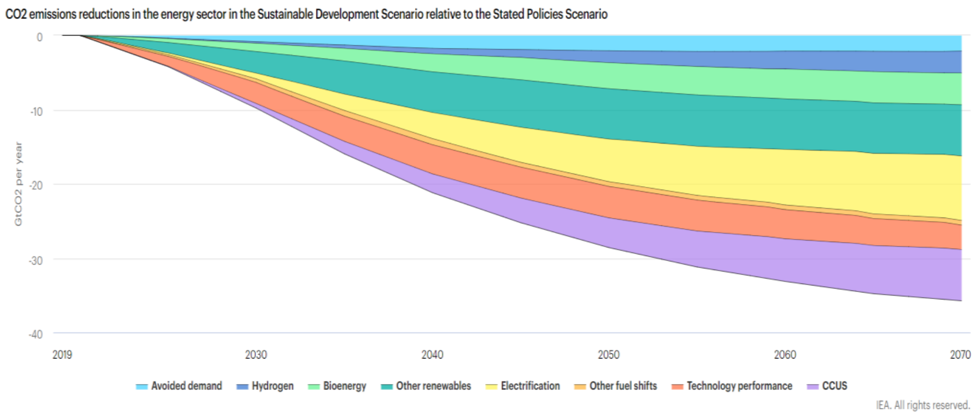

Figure 3 Cumulative emissions reduction.

1. Carbon Capture and Storage

As its name indicates, Carbon capture and storage is a technology that consists of capturing CO_2 directly from large sources like industrial facilities or power plants. Then the CO_2 captured is transported by pipelines, trucks… to be injected in deep formations for long-term storage.

The first CO_2 storage projected dedicated to reducing emissions (not for EOR) was in Norway, at the Sleipner gas fields, in 1996. Carbon capture and storage (CCS) is expanding rapidly, in fact, as of July 31, 2023, CCS projects in the public domain have a total CO_2 capture capacity of 361 Mtpa, over 50% more than the one of 2022.

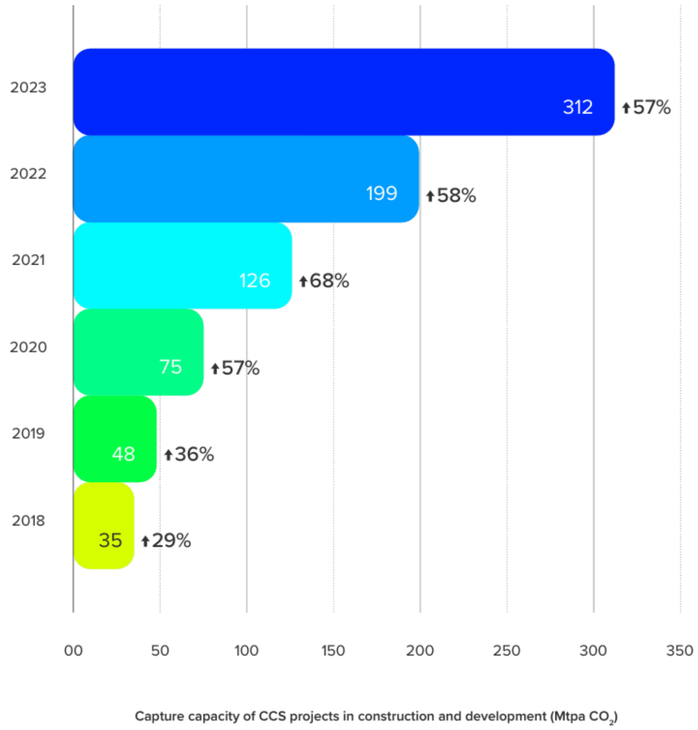

Figure 4 Growth of Capture Capacity of CCS [12]

2. Underground storage types

In general, to be considered a suitable underground storage site, the geological formation must have:

- High Capacity: the site should contain significant porosity (ϕ>20%) and/or occupy a very large area.
- Adequate injectivity: the formation possesses high permeability ensuring that lower wellhead pressures can be used to maintain desired injection rates.
- A satisfactory sealing caprock: to ensure that the injected CO_2 does not escape to the surface or leak into groundwater.
- Sufficient stable geological environment to ensure site integrity.

CO_2 storage types can be divided into 3 main categories: saline aquifer formations, depleted oil and gas reservoirs and unmineable coal beds.

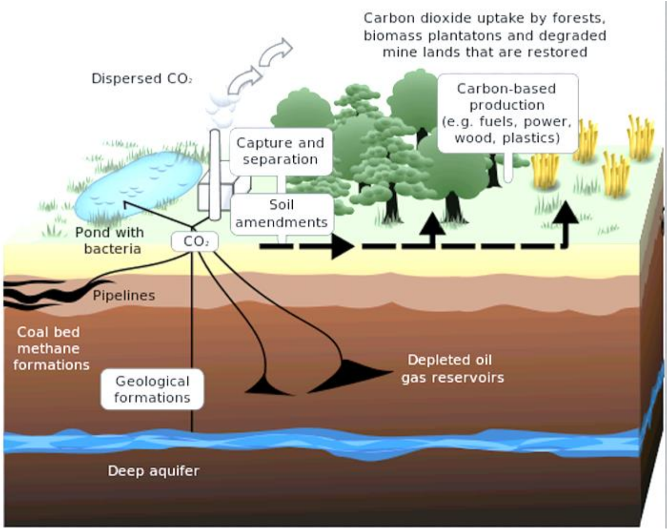

Figure 5 CCS storage types

- Depleted gas and oil reservoirs

A reservoir is considered to be depleted when it is no longer economically viable for hydrocarbon production, in other words, no longer possible to extract hydrocarbons. These reservoirs are prime candidates for CO_2 storage for several reasons:

In fact, oil and gas have been originally accumulated and retained in these reservoirs for millions of years which demonstrates the containment and the integrity of the reservoir, however, it's important to ensure that extraction wells didn't cause any damage that can cause a leakage pathway for CO_2.

Additionally, these sites were already well characterized for the production phase and all physical and structural properties have been extensively studied, which can reduce data acquisition costs.

Most of these oil and gas reservoir rocks are made of sandstone, limestone, and dolomite, and they have enough porosity and permeability to support huge CO_2 volume injections. They also feature well-defined low permeability caprocks, such as shale, anhydrite, or tight carbonates, which restrict leaking into shallower strata. However, not all depleted reservoirs are equally suitable for CO_2 injection. Factors such as rock type, porosity, permeability, and fluid properties can influence the feasibility and effectiveness of CO_2 storage.

Moreover, from the infrastructure side, existing wells and platforms can be potentially reused, which helps in reducing construction costs but also the condition of the wells should be assessed.

From the storage capacity point of view, for hydrocarbon reservoirs with small water encroachment (small aquifer), the injected CO_2 will generally occupy the pore volume previously occupied by oil and/or natural gas. However, not all the pore space will be available for CO_2 because some residual water may be trapped in the pore space due to capillarity, viscous fingering effects [11]

For large aquifer support reservoirs, where pressure is maintained by water influx, in addition to the capacity reduction caused by capillarity and other effects, a significant fraction of the pore space will be invaded by water, decreasing the pore space available for CO_2 storage, considering that repressuring the reservoir is limited to preserve reservoir integrity.

- Saline aquifer formations

Saline aquifers consist of deep sedimentary rocks saturated with saline water in their pore spaces, commonly known as brine, containing high concentrations of dissolved salts, making it unsuitable for irrigation or consumption.

These formations are widespread and contain vast quantities of brine. Consequently, they offer significant potential for large-scale carbon dioxide storage, particularly in regions lacking depleted hydrocarbon reservoirs.

Despite their extensive distribution and substantial storage capacity, saline aquifers have historically received less attention than hydrocarbon reservoirs, since they lead to uncertainties regarding containment security and fluid flow properties. In addition, the usable capacity of these resources is initially unknown because there is insufficient site-specific data to characterize them.

Saline aquifers can be classified into two types: confined and unconfined (open boundary conditions). Confined aquifers, like oil and gas reservoirs, enclose fluid inside structural (e.g., anticlines) or stratigraphic (e.g., pinch outs) geological features. These aquifers provide vertical and lateral confinement but have reduced storage capacity compared to unconfined aquifers where fluid may travel freely laterally.

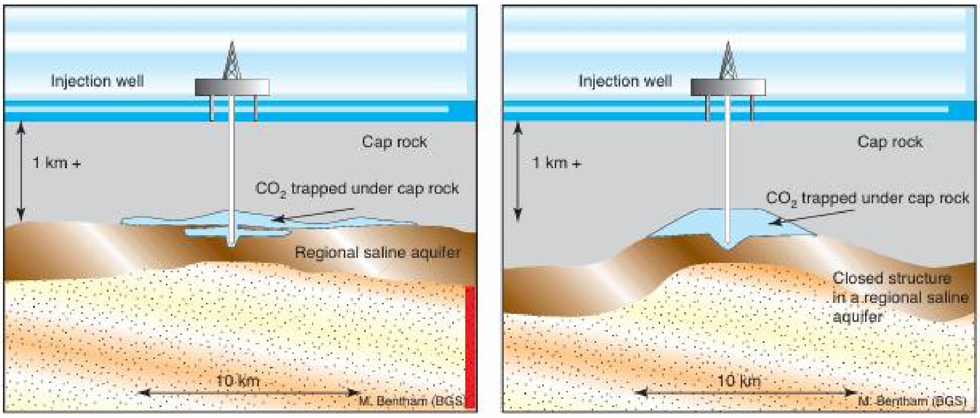

Figure 6 Unconfined and confined saline aquifers.

- Unmineable coal beds:

Carbon dioxide is stored in coal beds by adsorption rather than pore space filling. CO_2 is preferentially adsorbed, displacing methane from the coal. As with EOR, this technique may be utilized to produce coal bed methane, allowing CO_2 storage to be integrated with hydrocarbon production.
An advantage of this process is that a large amount of CO_2 can be stored at relatively low pressure, thereby reducing the cost of pumping and injection.

Reservoir type	Lower estimate of storage capacity ($GtCO_2$)	Upper estimate of storage capacity ($GtCO_2$)
Oil and gas fields	675[a]	900[a]
Unminable coal seams (ECBM)	3-15	200
Deep saline formations	1000	Uncertain, but possibly 10^4

[a] These numbers would increase by 25% if "undiscovered" oil and gas fields were included in this assessment.

Figure 7 Storage capacity for several geological storage options

3. Trapping mechanisms

CO_2 storage capacity and injectivity rely on geological and petrophysical properties that depend on the target formation. The injected CO_2 is trapped underground due to two main types of trapping mechanisms: physical and geochemical. In fact, the effectiveness of long-term storage will rely on these mechanisms.

- Physical trapping mechanisms
  1) Structural/ Stratigraphic trapping

It's considered the first type of trapping encountered by CO_2 underground. It consists of geological seals with low permeability (caprocks) such as low permeability shales, faults… that form a barrier for the CO_2 while it's migrating upwards due to its buoyancy: density gradient - CO_2 density is lower than the formation fluid. After reaching the caprock, the CO_2 tends to flow laterally as well until a cap rock, fault or other sealed discontinuity is reached. This trapping mechanism is the most dominant in depleted oil and gas fields.

This type of trapping is in fact crucial for qualifying a given formation to be considered a storing site because the structural and stratigraphic trapping is the main mechanism that prevents CO_2 leakage through the top layer [26].

There are numerous variations of structural and stratigraphic traps, or combinations of both structural and stratigraphic traps that can be physical traps for geological CO_2 storage. The trapping efficiency is determined by the structure of the sedimentary basins, which have an intricate plumbing system defined by the location of high and low permeability strata that control the flow of fluids throughout the basin. [24]

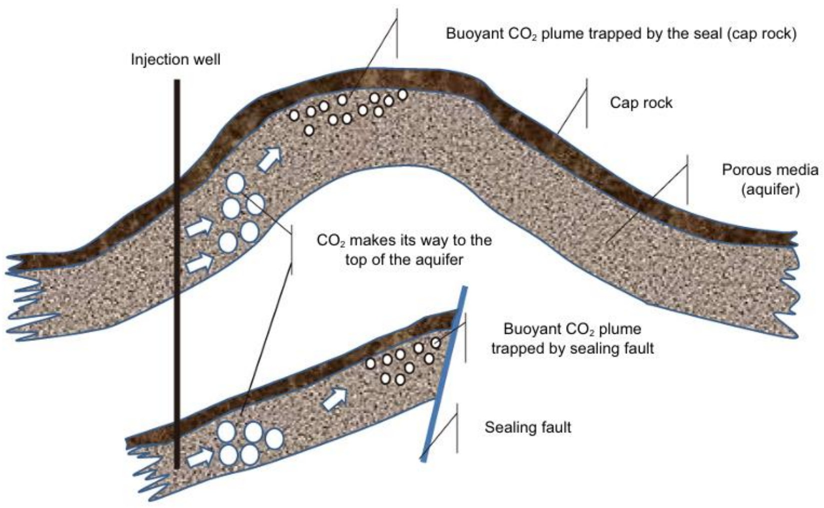

Figure 8 Structural trapping of injected CO_2 as a result of the formation structure. [13]

2) Residual trapping

When CO_2 is injected into a deep underground geologic formation, it displaces the resident fluid, which is often brine or in some cases hydrocarbons, and after stop of the injection, CO_2 migrates upward and laterally in response to buoyancy and pressure gradients. The brine displaces CO_2 and reservoir fluid fills the left spots, but some CO_2 droplets are left behind in pore spaces. So, these disconnected CO_2 droplets are then trapped in the pores of the reservoir as immobile phase.

This trapping mechanism can be also called capillary trapping. It has a very strong effect on the migration and distribution of CO_2 in the reservoir and can affect the contribution of the other mechanisms to the trapping process.

Residual trapping efficiency is influenced by the properties of the rock formation, such as porosity, permeability, and pore size distribution. It is considered one of the mechanisms providing long-term storage solution since once CO_2 is trapped in the rock pores, it is effectively immobilized and unlikely to migrate.

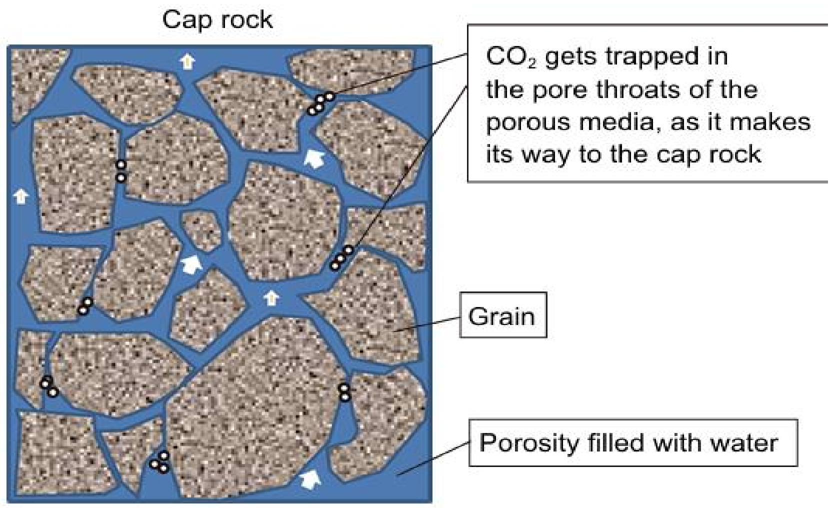

Figure 9 Residual trapping of CO_2 [13]

- Geochemical trapping mechanisms

1) Solubility trapping

When CO_2 is injected into a porous rock formation, it initially exists as a separate supercritical (or gaseous) phase as already discussed. However, over time, CO_2 comes into contact with the formation water and begins to dissolve into it, forming a single-phase mixture, resulting in densely saturated brine. At this stage, it no longer exists as a separate phase, which means no buoyancy effect. CO_2-saturated brine becomes denser than reservoir fluids and settles to the formation's bottom due to gravity, resulting in stronger CO_2 trapping over time.
This method of CO_2 sequestration enhances the security and permanence of CO_2 storage, as the dissolved CO_2 is less likely to escape from the storage site.
Moreover, the solubility of CO_2 in water is dependent on the pressure, temperature, salinity and chemical properties of the formation water.
Dissolution of CO_2 in brine equation:

$$CO_2 + H_2O \leftrightarrow H_2CO_3$$

This process is very slow because the molecular diffusion coefficient is very small. It will take thousands of years for CO2 to be completely dissolved in brine. [24]

2) Ionic trapping

CO_2 has dissolved in formation brine and form carbonic acid (H_2CO_3), later deprotonations produce the bicarbonate ion (HCO_3^-) and the carbonate ion (CO_3^{2-}):

$$H_2CO_3 + OH^- \leftrightarrow H_2O + HCO_3^-$$

$$HCO_3^- + OH^- \leftrightarrow H_2O + CO_3^{2-}$$

The amount of CO_2 trapped by ionic trapping is strongly dependent on the quantity of CO_2 already dissolved in the brine and on the brine pH and the brine ionic composition as well, which governs the dissociation reactions. Ionic trapping occurs for pH greater than 6, when most of the dissolved carbon is in an ionic state rather than as carbonic acid and aqueous CO_2.

3) Mineral trapping

Mineral trapping mainly consists of the reaction of CO_2 with solid minerals (Ca, Fe, Mg) contained in the rock matrix and results in the precipitation of carbonates in the pore space and so incorporating CO_2 in a stable mineral phase via reactions with the minerals and the organic matters.

$$CO_2 + Ca^{2+} + H_2O \leftrightarrow CaCO_3 + 2H^+$$

$$CO_2 + Mg^{2+} + H_2O \leftrightarrow MgCO_3 + 2H^+$$

$$CO_2 + Fe^{2+} + H_2O \leftrightarrow FeCO_3 + 2H^+$$

This mechanism is the slowest one, operating in a significant way on a millennial time scale under subsurface conditions, but is the one process that leaves CO_2 in a completely immobile state, so it is considered the most secure process since the formation of solid carbonate minerals provides a permanent and stable form of CO_2 storage, preventing any future release.

This trapping mechanism depends mainly on the rock minerals, as well as on the pressure of the gas, temperature and porosity and has been found to produce significant changes in the rock permeability and porosity due to the precipitation of carbonates.

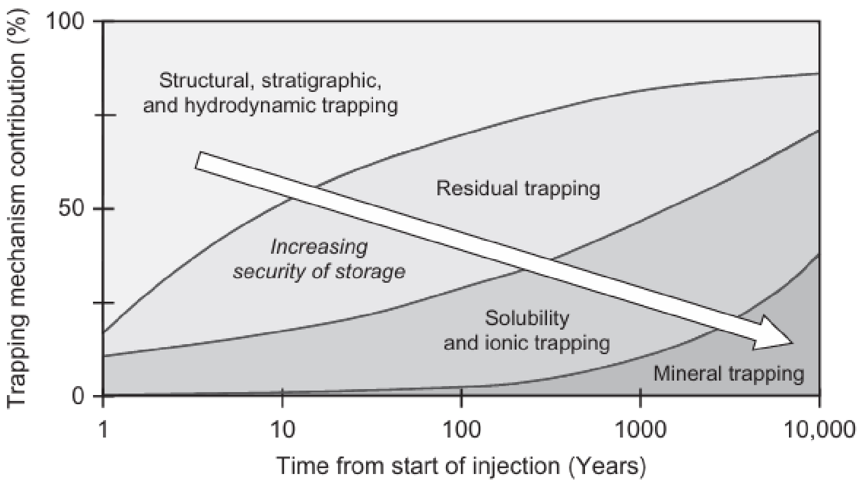

Figure 10 Trapping mechanisms contribution through time

4. Underground CO_2 behavior

To achieve an efficient underground carbon geological storage, understanding the chemical and thermodynamic conditions is crucial.
In general, CO_2 changes its state into a solid, liquid, gas, or supercritical state at specific temperatures and pressures as it is shown in the following diagram.

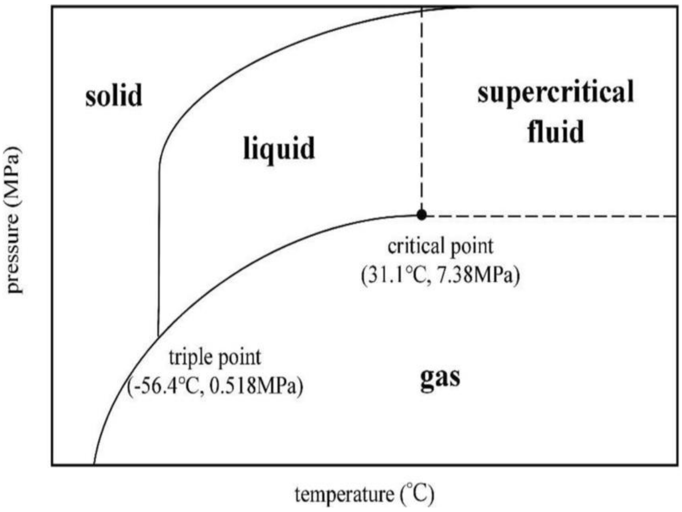

Figure 11 CO_2 phase diagram.

As evident from the graph, at 31.10 ◦C and 7.38 MPa, a critical point occurs in the CO_2 phase behavior. Above these pressure and temperature conditions, CO_2 changes into supercritical fluid state where CO_2 establishes the behavior of both gas and liquid phases, in fact, it has a density similar to a liquid but exhibits gas-type viscosity and behavior. Accordingly, CO_2 in supercritical state is a fluid with high mobility and significant density at the same time [28], that being so, supercritical CO_2 leads to more efficient storage.

Moreover, the preferred depth for CO_2 injection in order to increase storage safety is >800m, and at these depths and below, CO_2 is expected to be in supercritical state.

The table below summarizes the supercritical state of CO_2 during injection and storage.

CO_2 Supercritical State Conditions	**Values**
Temperature	31 °C
Pressure	7.38 MPa
Density	850 Kg/m^3
Depth	Below 800 m

Table 1 CO2 supercritical phase conditions

CO_2 phase behavior and physical properties like density, viscosity are immensely pressure and temperature dependent as shown in the following graphs. In fact, the behavior of density and viscosity with pressure and temperature is a key factor in implementing CO_2 underground storage capacity and injectivity which will he discussed later in this study.

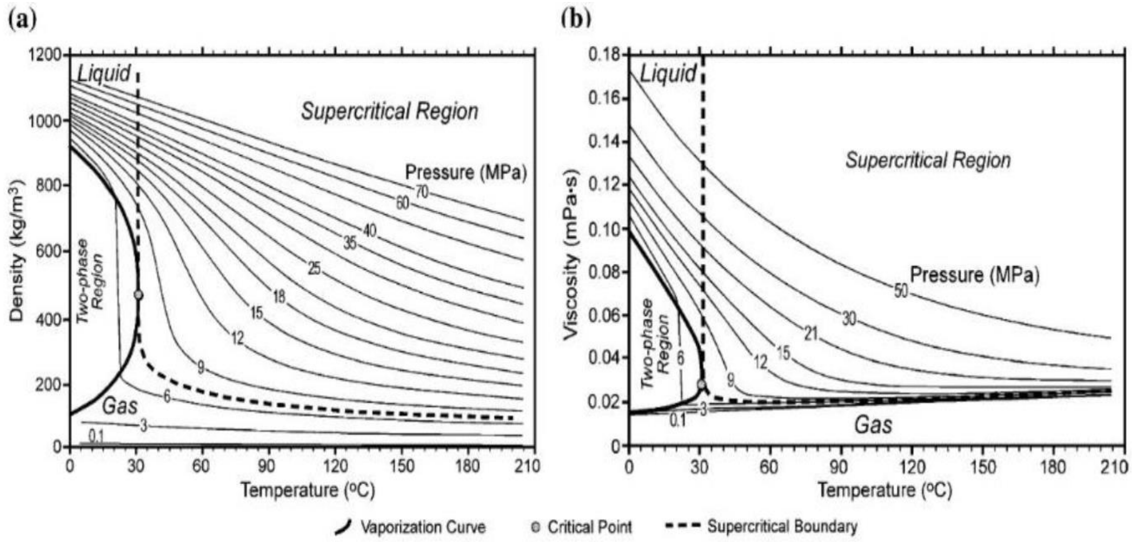

Figure 12 CO_2 density and viscosity in function of Pressure and Temperature [22]

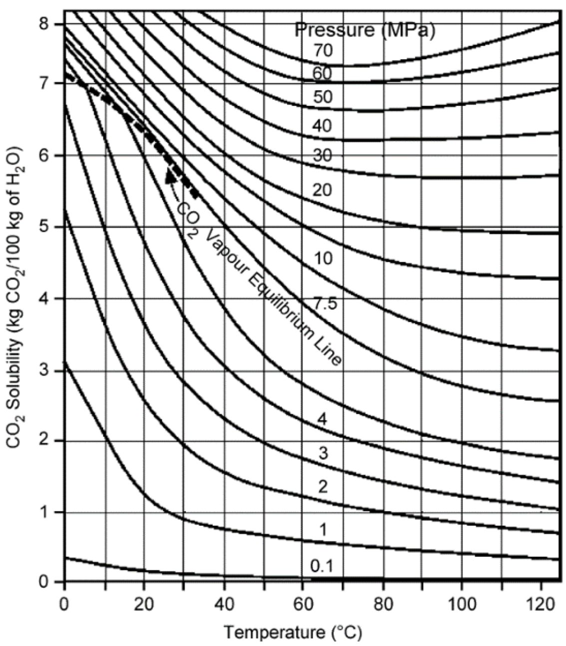

Figure 13 CO_2 solubility in function of pressure and temperature [22]

Regarding chemical properties, the level of solubility of CO_2 is variable depending on the specific pressure and temperature conditions. As we can see in the graph, CO_2 solubility increases with increasing pressure, but decreases with increasing temperature [21]. Its solubility in water also decreases with increasing water salinity due to the "salting-out" effect, where dissolved salts reduce the amount of CO_2 that can be dissolved in the water, in fact, the effect of water salinity on CO_2 solubility has a vital role in the solubility trapping potential of CO_2 in water bearing reservoirs, as mobile or connate water.

5. Numerical simulation and modeling

Numerical modeling stands as a fundament in the domain of carbon capture and storage, crucial for simulating and predicting the physical, chemical, and geomechanical processes involved in storing CO_2 underground. As already discussed, carbon storage projects include diverse types of underground basins, each presenting unique challenges for CO_2 storage. Moreover, various trapping mechanisms take place during these processes each playing a critical role in securely immobilizing CO_2 underground. Nevertheless, the interaction and combined impact of these mechanisms significantly amplify the complexity of CCS projects, necessitating advanced simulations that can effectively account for their simultaneous influence. In fact, the single contribution of each individual mechanism is also difficult to assess as CO_2 trapping largely depends not only on the fluid-rock mineral properties of the reservoir or aquifer under consideration but also on the CO_2 injection strategy; furthermore, each trapping mechanism is dependent on each other. [24]

Thus, numerical simulation software tools are indispensable in this regard, offering specialized capabilities to model multiphase fluid flow, geochemical reactions, and geomechanical responses within heterogeneous subsurface environments. For instance, tools like TOUGH2, CMG-GEM, and ECLIPSE are tailored to simulate CO_2 behavior under different reservoir conditions and injection strategies.

In this study, the simulations will be run using the commercial geochemical simulator Computer Modelling Group's CMG-GEM.

CMG-GEM is an efficient, multidimensional, equation-of- state (EOS) compositional simulator which can simulate all the important mechanisms of a miscible gas injection process. The software utilizes either the Peng-Robinson [ref] or the Soave- Redlich-Kwong [ref] equation of state to predict the phase equilibrium compositions and densities of the oil and gas phases and supports various schemes for computing related properties such as oil and gas viscosities. Moreover, it integrates geochemical processes, allowing for the simulation of reactions between CO_2, water, and reservoir rocks. This capability is vital for predicting long-term storage stability and the formation of carbonate minerals.

II. Models' characterization

This study focuses on the northern and central part of the Adriatic Sea. The main sedimentary inputs of the North-Central Adriatic Sea are located along the western side.

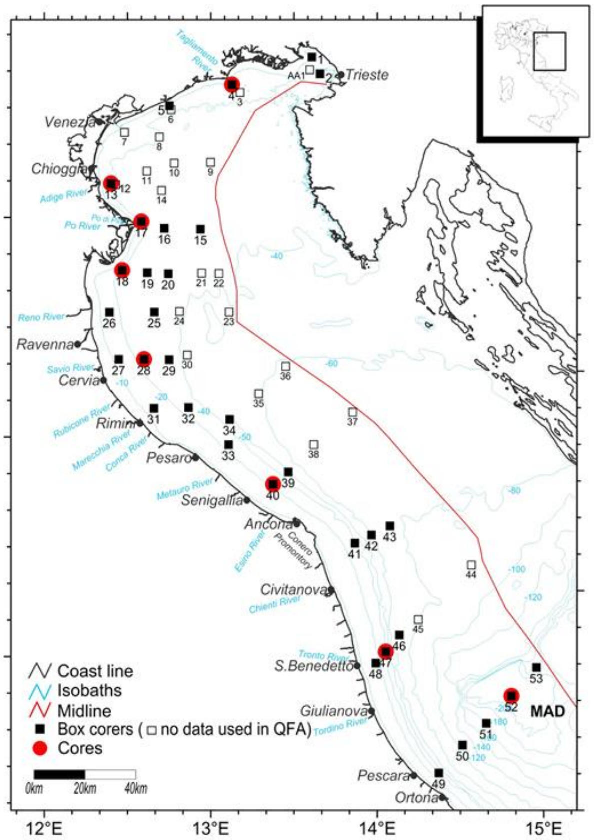

Figure 14 map representing the Adriatic Sea. [18]

1. Models' description

The models simulated in this study are based on statistical data of reservoirs in the region.

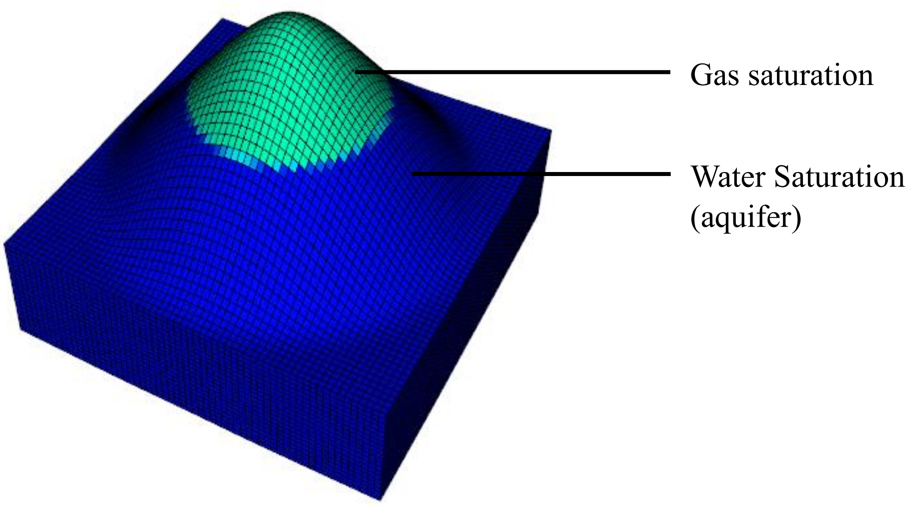

Figure 15 3D representation of model A

A 3D Conic grid was applied to generate an anticline reservoir geometry structure for each model with n_i=61, n_j=61, n_k=20 (number of blocks in each direction) so a total of 74420 blocks. Considering that the top grid depth differs according to the depth of each reservoir (1000, 2000, 3000 m).

A Carter-Tracy aquifer with the leaking option enabled was included with different dimensions (different rd/re ratio) in order to simulate the aquifer with a flowing boundary to each model.

2. Rock fluid parameters

As already mentioned, these models represent the various reservoirs in the region. Consequently, the parameters specifying the properties of the base case model are based as well on the average value of each parameter in the region. The following average parameters were used for the base case model:

Parameter	**Value**
Medium Porosity	20%
Mean Swi	30%
Avg. K abs	50 mD
Kv	5 mD
Kh	50 mD
Med. Hydrostatic grad.	0.104 bar/m
Med. Thermal grad.	3.25 °C /100m

Table 2 Average parameters value

However, according to depth, some properties and PVT parameters as well change. In the following table we will be presenting the different parameters according to the depth:

	1000 m	**2000 m**	**3000 m**
Pi (barsa)	103.9	207.79	311.69
T (°C)	32.47	64.94	97.40
C_w (1/bar)	3,7742E-05	3,9901E-05	4,2320E-05
C_f (1/bar)	5,5463E-05	2,6231E-05	1,6772E-05
C_{tot} (1/bar)	9,3206E-05	6,6132E-05	5,9093E-05
Density Water (sc kg/m3)	1021.7	1021.7	1021.7
Gas specific gravity	0.556188	0.556188	0.556188

Table 3 Rock-fluid properties (according to depth)

The water properties and composition are summarized in the following table. The dataset was retrieved from well logs data.

1000m		*2000 m*		*3000 m*	
pH	*7.01*	*pH*	*7.13*	*pH*	*7.13*
NaCl (g/l)	*23.638*	*NaCl (g/l)*	*34.901*	*NaCl (g/l)*	*34.901*
Water composition (mg/Cl)		*Water Composition (mg/l)*		*Water Composition (mg/l)*	
Na^+	8375	Na^+	12409	Na^+	12409
K^+	63	Cl^-	21173	Cl^-	21173
Ca^{2+}	317	K^+	177	K^+	177
Mg^{2+}	538	Ba^{2+}	16	Ba^{2+}	16
Ba^{2+}	2.1	Ca^{2+}	472	Ca^{2+}	472
Sr^-	13.5	Mg^2	554	Mg^2	554
Fe^{2+}	8.4	Br^-	99	Br^-	99
NH_4^+	60	Sr^-	19	Sr^-	19
SiO_2	12.2				
Cl^-	14339				
SO_4^{2-}	390				
$NaHCO_3$	458				

Table 4 Water properties

The relative permeability curves considered for the base case are as follows:

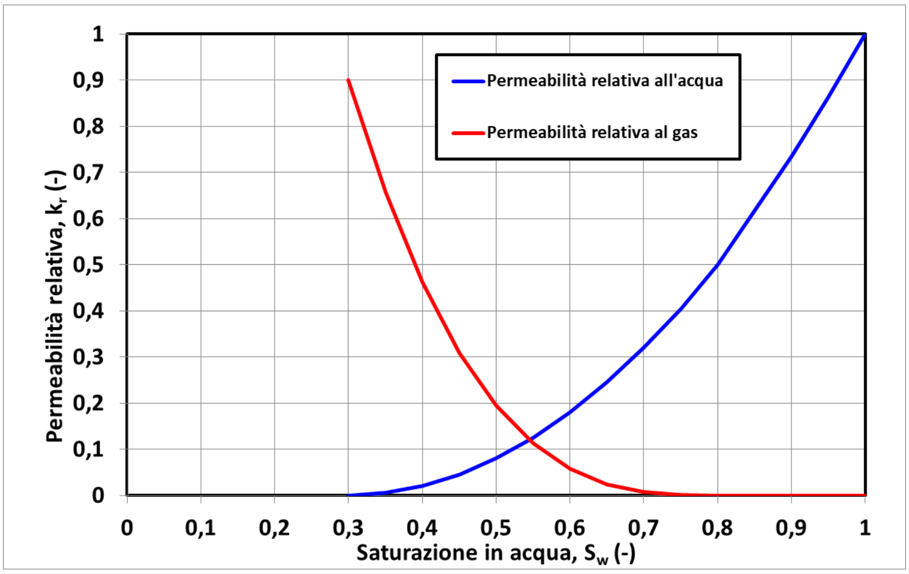

Figure 16 Relative permeability curves-base case

The curves were defined based on the Corey-Brooks method with nrw=2, nrg=3, nrw_{aq}=2, Swi=0.3, Sgt=0.2, and the following end points: Krw_{sgt}=0.5, Krw_{max}=1, Krg_{swi}=0.9.

3. Geochemistry

CO_2 solubility with the formation water was considered in this model. GEM uses the modified Henry's constant [ref] to model CO_2 solubility. The Henry constant is dependent on pressure, temperature and salinity.

As discussed, the mineralogy of the site has a direct impact on the mineral trapping mechanism. The main minerals present in the site are summarized in the following table:

Mineralogy	**Initial Volume fraction (%)**
Quartz	21.9
Calcite	13.15
Aragonite	7.1
Albite	3.1
Anorthite	8.5
K- feldspar	3.1
Muscovite	15.5
Chlorite	1.5
Chamosite	1.5
Dolomite	12.9
Siderite	13.15
Illite	1.1
Kaolinite	2.7
Halite	1

Table 5 Minerals fractions

The aqueous reactions mentioned previously were added:

$$H_2O + CO_2 \leftrightarrow H^+ + HCO_3^-$$

$$CO_3^- + H^+ \leftrightarrow HCO_3^-$$

The water dissociation equation as well:

$$OH^- + H^+ \leftrightarrow H_2O$$

As well as the mineralization reactions of CO2 with the mentioned minerals:

$$'Quartz' \leftrightarrow SiO_{2(aq)}$$

$$'Calcite' + H^+ \leftrightarrow HCO_3^- + Ca^{2+}$$

$$'Aragonite' + H^+ \leftrightarrow HCO_3^- + Ca^{2+}$$

$$'Albite' + 4H^+ \leftrightarrow 3SiO_2 + Al^{3+} + Na^+ + 2\,H_2O$$

$$'Anorthite' + 8H^+ \leftrightarrow 2SiO_2 + 2Al^{3+} + Ca^{2+} + 4\,H_2O$$

$$'K - \text{feldspars}' + 4H^+ \leftrightarrow 3SiO_2 + Al^{3+} + K^+ + 2\,H_2O$$

$$'Muscovite' + 10H^+ \leftrightarrow 3SiO_2 + 3\,Al^{3+} + K^+ + 6\,H_2O$$

$$'\text{Chlorite}' + 16H^+ \leftrightarrow 3\,SiO_2 + 2\,Al^{3+} + 5\,Mg^{2+} + 12\,H_2O$$

$$'Chamosite' + 10\,H^+ \leftrightarrow\; SiO_2 + 2\,Fe^{2+} + 2\,Al^{3+} + 7\,H_2O$$

$$'Dolomite' + 2\,H^+ \leftrightarrow 2HCO_3^- + Mg^{2+} + Ca^{2+}$$

$$'Siderite' +\; H^+ \leftrightarrow HCO_3^- + Fe^{2+}$$

$$'\mathrm{Illite}' + 8\,H^+ \leftrightarrow 3.5\,SiO_2 + 0.6\,K^+ + 2.3\,Al^{3+} + 0.25\,Mg^{2+} + 5\,H_2O$$

$$'\mathrm{Kaolinite}' + 6\,H^+ \leftrightarrow 2\,SiO_2 + 2\,Al^{3+} + 5\,H_2O$$

$$'\mathrm{Halite}' \leftrightarrow\; Cl^- + Na^+$$

Reaction	***a0***	***a1***	***a2***	***a3***	***a4***	***area0 (m^2/m^3)***	***E_act (J/mol)***	***K0_ref (mol/m^2s)***	***T_ref(°C)***
Quartz	*-4.49*	*0.022*	*-1e-4*	*3e-7*	*-4e-10*	*2650*	*90900*	*-13.4*	*25*
Calcite	*2.07*	*-0.014*	*-6e-6*	*1e-7*	*-4e-10*	*2709.95*	*14400*	*-0.3*	*25*
Aragonite	*2.24*	*-0.015*	*-5e-6*	*1.5e-7*	*-4e-10*	*8807.34*	*71200*	*-7.7*	*25*
Albite	*3.92*	*-0.034*	*2.5e-5*	*3e-7*	*-8e-10*	*2384.2*	*65000*	*-10.16*	*25*
Anorthite	*31.75*	*-0.2*	*6e-4*	*-9e-7*	*9e-11*	*2760*	*17800*	*-9.12*	*25*
K-feldspar	*0.46*	*-0.015*	*-3.9e-5*	*4e-7*	*-9e-10*	*2329.6*	*51700*	*-10.06*	*25*
Muscovite	*18.25*	*-0.16*	*4.5e-4*	*-4.8e-7*	*-5e-10*	*1776.7*	*54391*	*-6.44*	*37.6*
Chlorite	*78.3*	*-0.42*	*1.3e-3*	*-2e-6*	*5.4e-10*	*7020*	*88000*	*-11.11*	*25*
Chamosite	*39*	*-0.25*	*7e-4*	*-1.35e-6*	*4e-10*	*7020*	*88000*	*-11.11*	*25*
Dolomite	*3.39*	*-0.036*	*1.32e-5*	*2.41e+7*	*-8e-10*	*2864.9*	*52200*	*-7.53*	*25*
Siderite	*0.25*	*-0.02*	*9.5e-6*	*1e-7*	*-4e-10*	*4046.67*	*52200*	*-7.53*	*25*
Illite	*12.43*	*-0.11*	*2e-4*	*-8e-8*	*-8e-10*	*2763.07*	*35000*	*-12.78*	*25*
Kaolinite	*9.73*	*-0.09*	*3e-4*	*-3e-7*	*-3e-10*	*2594.05*	*22200*	*-13.18*	*25*
Halite	*1.5*	*0.004*	*-6e-5*	*2.2e-7*	*-4e-10*	*2163.35*	*7400*	*-0.21*	*25*

Table 6 Reactions parameters

III. Production phase

Regarding the depletion of the reservoirs, the production phase for each model occurs from 1/12/1979 till 1/1/2010. For the models A, B, C, F, G…. two production wells have been used for the depletion process, for model D, one well and for the model E four wells and this depends on the GOIP. All the wells used are vertical wells with rw=0.0889 m, geometric factor of 0.37, wfrac=1 and skin=5.

The following table summarizes the well pressure and rate constraints operating the wells during production of the base case A, considering that the values mentioned below are defined per well:

Constraint (base case)	
Min WHP	4000 KPa
Min BHP	1000 Kpa
Max STG	250 000 m^3/day
Min STG	20 000 m^3/day
WGR	0.00001
STG	0.9

Table 7 Well constraints (case A)

The rate and Pressure profile related to the production phase of the base case are as follows:

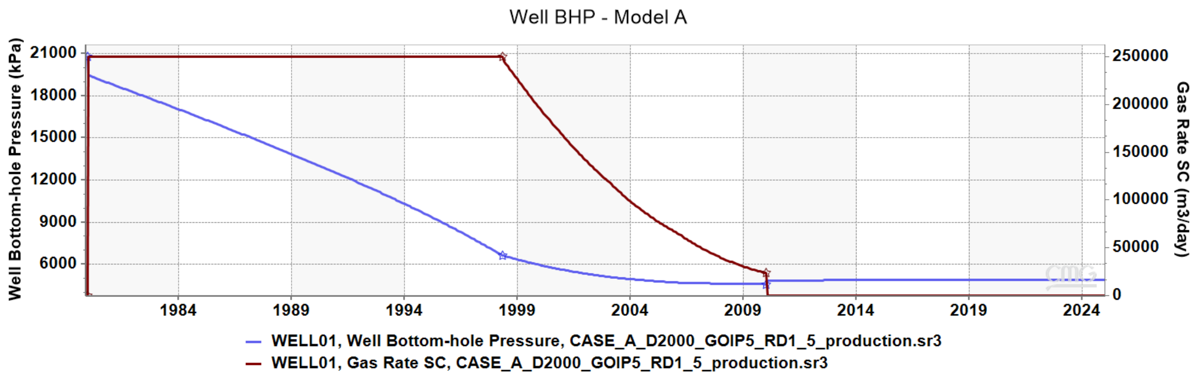

Figure 17 Production Case A- pressure profile

IV. Injection phase

As we already mentioned, model A is considered as the base model, with 2000 m depth, rd/re=1.5 and GOIP =5G Sm^3. All the parameters defining the model were mentioned in the previous chapter.

After the depletion phase, the production wells were shut down for 15 years and then the injection phase is modelled to initiate on the 1/1/2025.

Same wells are used for the injection phase, with the following constraints:

- max BHP of 20779 Kpa which is the initial pressure of the reservoir
- maximum difference between the wellbore pressure and the grid block pressure of 3000 Kpa and a maximum rate of 400000 m^3/day. Thus, no constant rate was defined for the injection, thus, the rate was defined by this maximum difference of pressure.

After injection, simulation was run for more years to be able to track the long-term changes in the pressure dissipation and trapping mechanisms.

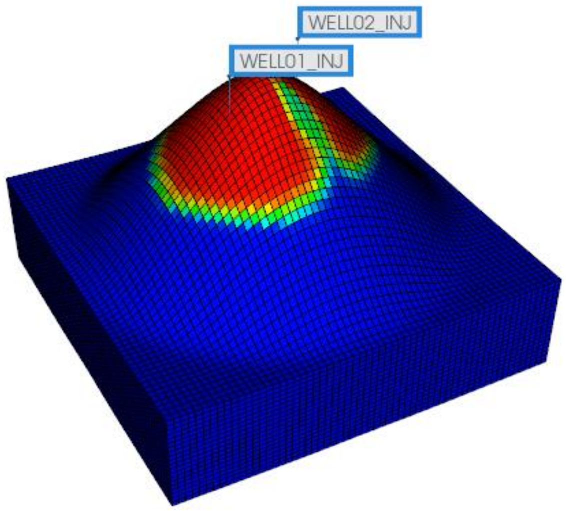

Figure 18 3D representation of model A after CO2 injection

In the following graph we can see the Pressure and rate profiles:

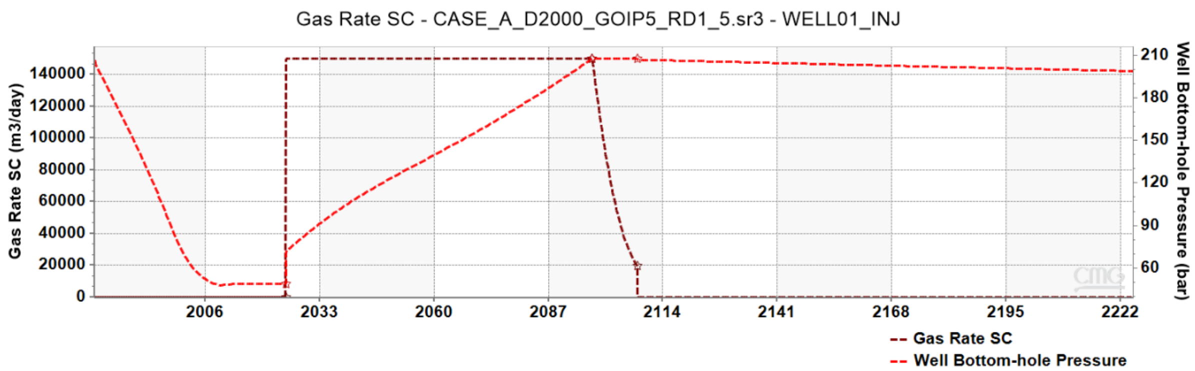

Figure 19 Injection phase- Case A

At the end of the injection, the total stored CO_2 is as follows:

Model	Depth (m)	Total CO2 stored (Kg)	Residual trapping	Solubility trapping	Structural trapping	Mineral trapping	Ionic trapping
A	2000	9.260263E+09	31.72 %	6.13 %	55.35 %	2.1 %	4.6 %

Table 8 Total CO2 stored-base case

The following plot defines the trend of the three trapping mechanisms in the reservoir:

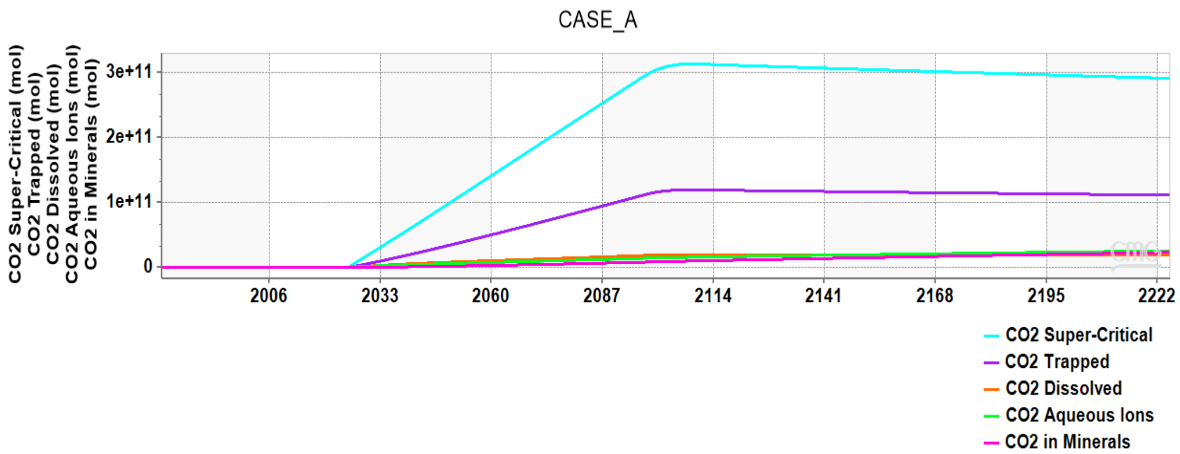

Figure 20 Different trapping mechanisms case A

V. Sensitivity analysis

To understand the impacts caused by different parameters on CO_2 storage, sensitivity analysis will be performed by varying different values corresponding to each parameter in question and examining the changes using different numerical simulations. For all the analyses, the total amount of CO_2 stored will be compared between the different models. Moreover, when discussing geological storage, it is crucial to understand which trapping mechanisms are prevalent in each case.

The following table summarizes all the sensitivities that will be performed with the different parameters:

Parameter	***Lower value***	***Mid Value***	***Upper value***	***Unit***
Depth	*1000*	*2000*	*3000*	*m*
GOIP	*1*	*5*	*10*	*B* m^3 *sc*
Aquifer size	*1.5*	*5*	*10*	-
Porosity	*0.15*	*0.2*	*0.25*	-
Sgr	*0.1*	*0.2*	*0.3*	-
Swi	*0.1*	*0.3*	*0.55*	-
Krco2	*0.3*	*0.6*	*0.9*	-
Kabs	*20*	*50*	*100*	*mD*
Kv/Kh	*0.1*	*0.5*	*1*	-
Injection rate	*200*	*300*	*400*	m^3*/day*
Ramp-up injection steps	*2*	-	*4*	*steps*

Table 9 Different sensitivities parameters

1. Reservoir Depth:

To study the influence of depth variation, three models representing the site at different depths will be analyzed. The base model, Model A, is situated at 2000 meters. For comparison, Model B is at 1000 meters, and Model C is at 3000 meters.

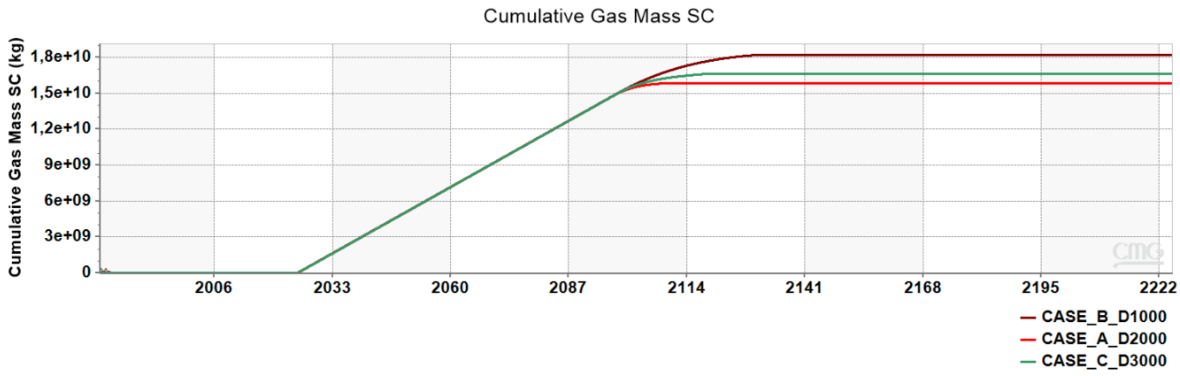

Figure 21 Cumulative gas trapped (different depths)

In the following table, detailed information about the amount of CO_2 captured are presented and a comparison for the different trapping mechanisms between the three models on 1 Jan 2155:

Model	Depth (m)	Total CO_2 stored (Kg)	Residual trapping	Solubility trapping	Structural trapping	Mineral trapping	Ionic trapping
B	1000	1.8E+10	30 %	5.8 %	60%	0.7 %	2.7%
A	2000	1.5E+10	33.2 %	5.5 %	53.7 %	3 %	4 %
C	3000	1.6E+10	26 %	5 %	33%	25 %	10 %

Table 10 Amount of CO_2 trapped by model A, B and C

With the variation in depth, the main characteristics that change are pressure and temperature. Therefore, while studying the depth variations in the three models, the impact of pressure and temperature on CO_2 storage will be analyzed. As previously outlined, the prevailing pressure and temperature of a reservoir significantly affect the properties of CO_2.

Considering that the three reservoirs have different temperature due to difference of depth and according to the thermal gradient mentioned in Table 2, the temperatures of the three reservoirs (B, A, C) are 32.47°C, 64.94°C, 97.4°C respectively.

Concerning the solubility of CO_2, as already discussed in the first part of this report, it increases with increasing pressure, but decreases with temperature. And as shown in our case, solubility is playing a less important role in trapping CO_2 with increasing depth. The percentage of CO_2 trapped due to the solubility of CO_2 is the highest for model B where we have the lowest temperature and lowest pressure. So, we can conclude that the temperature has a higher impact. But that doesn't mean that the pressure is not playing an important role as well, since the solubility trapping percentage is not widely changing between the three cases.

The following plane sections (Figures 22,23,24) highlight more the CO_2 dissolution increase with increasing depth, since it's clear that in case B (1000 m) more CO_2 has been dissolved.

The mineral trapping contribution is very low for shallow depth but increases with increasing in depth, as well as for sure the ionic trapping. In fact, higher temperatures can enhance the kinetics mineral reactions which leads to this high contribution of mineral trapping at large depth. Moreover, due to the high amount of CO_2 trapped by the mineral reactions, more amount of CO2 has been injected and this explains the total CO_2 mass stored which is very close to the base case.

As a consequence of the increase of potential of the mineral and ionic trapping, the residual trapping as well as the structural trapping mechanisms contribution decrease, due to the high amount of CO_2 in minerals and aqueous ions.

Concerning the mineral trapping, it was only studied in the first sensitivity related to the difference in depth. However, in the following sensitivities, the geochemistry will not be considered, first, since all the sensitivities will be based on case A, where the contribution of the mineral trapping is relatively small and is not affecting in a large way the other mechanisms.

Figure 22 CO_2 saturation - case B (1000 m)

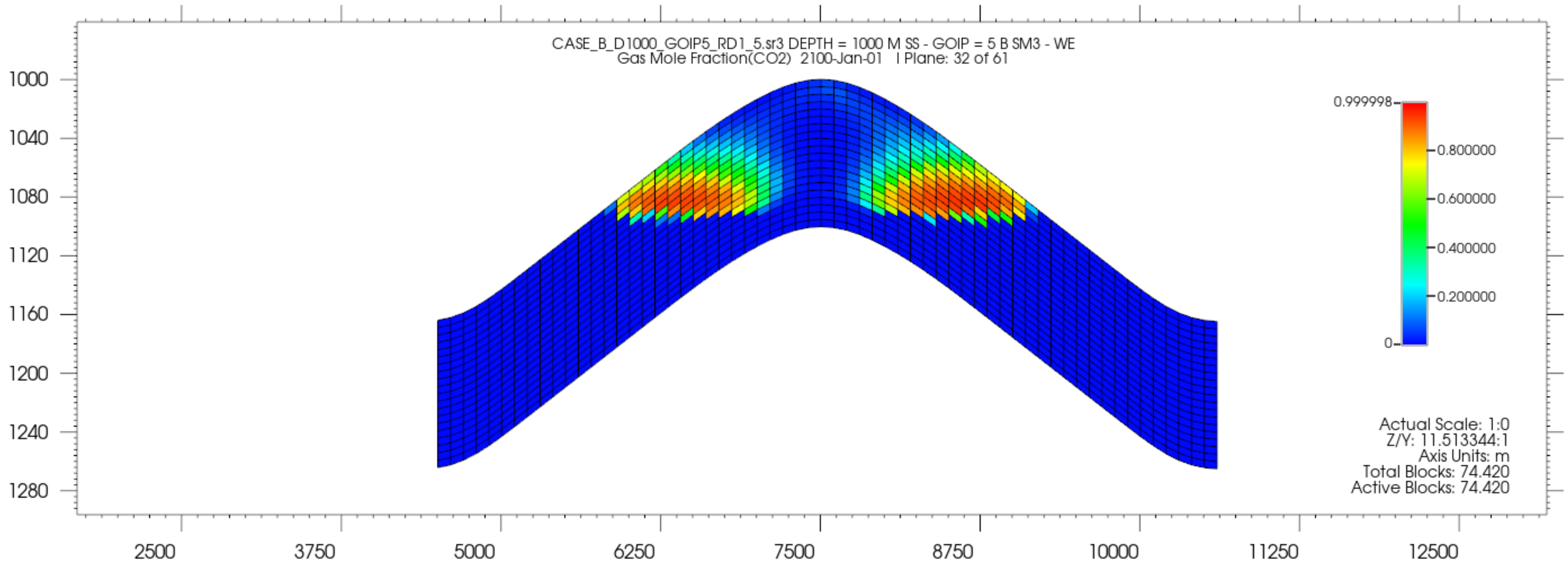

Figure 23 CO_2 saturation - case A (2000 m)

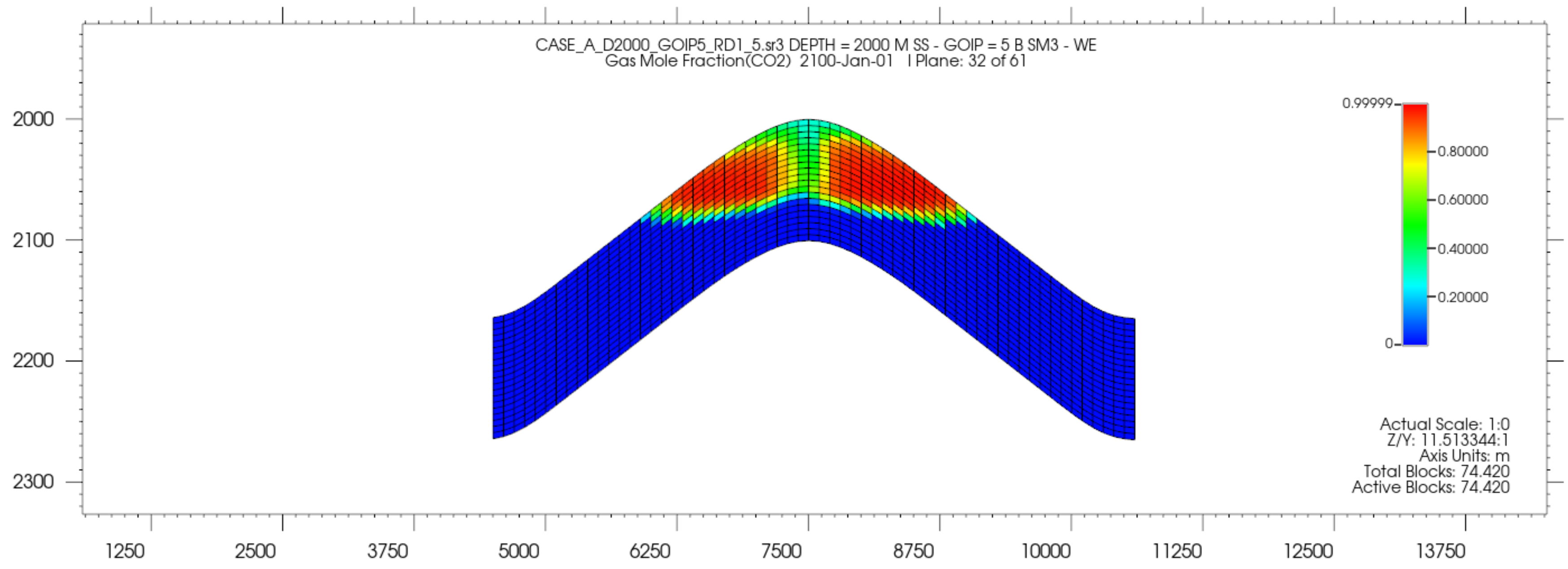

Figure 24 CO_2 saturation - case C (3000 m)

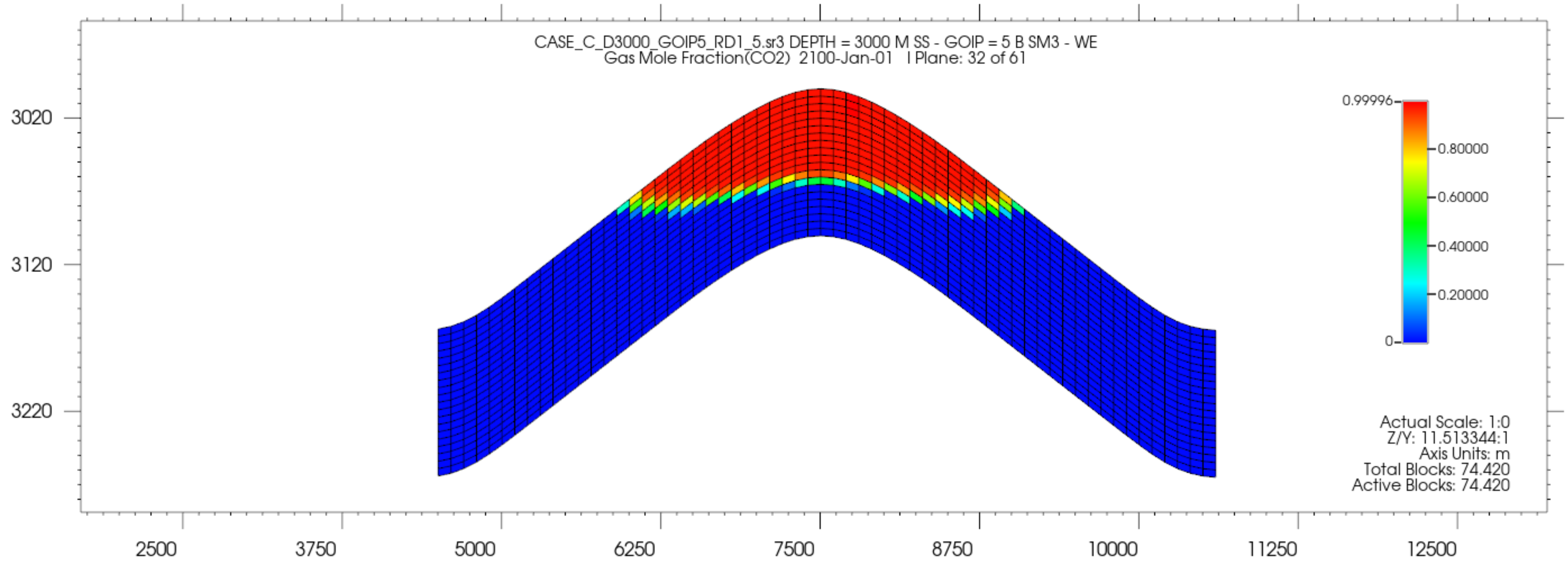

2. GOIP

To understand the importance of GOIP in CO_2 storage, the base case A (GOIP =5 B Sm^3) will be compared with a relatively low GOIP model (case D: GOIP = 1 B Sm^3) and large GOIP model (case E: GOIP = 10 B Sm^3).

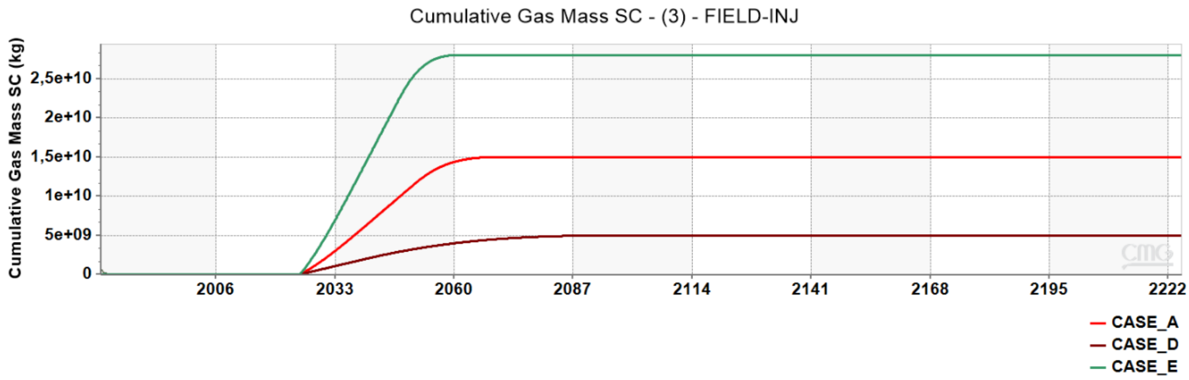

Figure 25 Cum. CO_2 stored (diff. GOIP)

Models	**GOIP (BSm^3)**	**Total CO2 captured (Kg)**	**Residual Trapping (%)**	**Solubility trapping (%)**	**Structural trapping (%)**
D	1	0.5E+10	30.81 %	6.06 %	63.1 %
A (base case)	5	1.5E+10	35.5 %	6.06 %	58.3 %
E	10	2.8E+10	31.56 %	4.44 %	64 %

Table 11 Amount of CO_2 trapped by different mechanisms (cases A, D, E)

The graph clearly shows the difference between the three cases, with the highest amount of CO_2 stored in Case E, which has the highest Gas Originally Initial in Place (GOIP). These results are logical since case E offers the largest storage capacity due to the significant amount of hydrocarbons initially present in the reservoir, allowing for the greatest capacity for CO_2 storage. This is also illustrated in Figures 26, 27, and 28.

Concerning the solubility trapping, it less contributes in case E, since the reservoir has the largest size, thus the ratio between aquifer size which is the same for the three cases and the reservoir size is very small compared to models A and D leading relatively to less water encroachment in this case thus, less water amount for CO_2 to be able to be dissolved in.

In the three cases, the structural trapping plays the dominant role in trapping CO_2 having the highest contribution in case E due to the largest reservoir size and thus the largest space for migration of free gas in the reservoir.

Figure 26 CO_2 injected-Case D

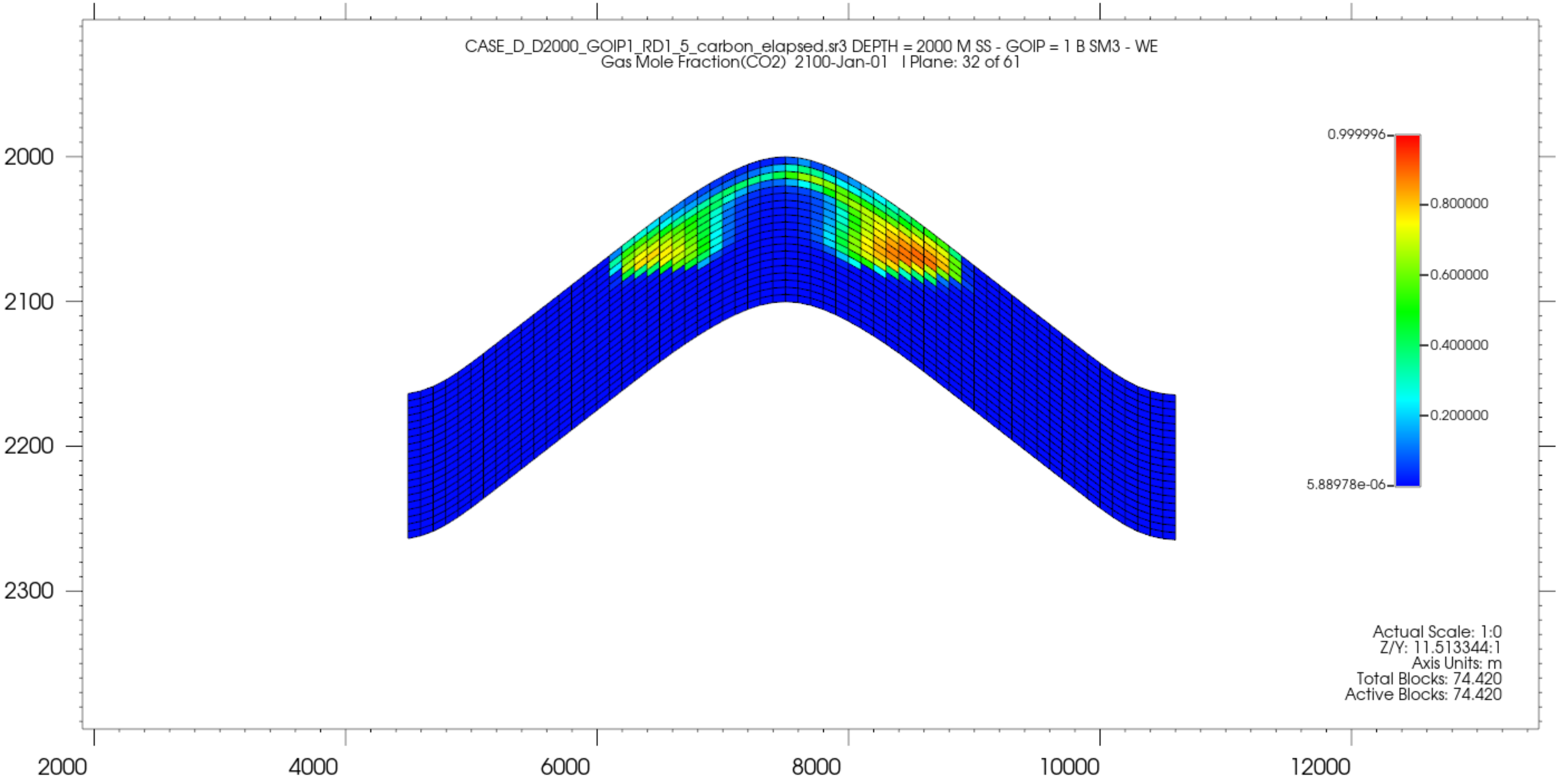

Figure 27 CO_2 injected- case A

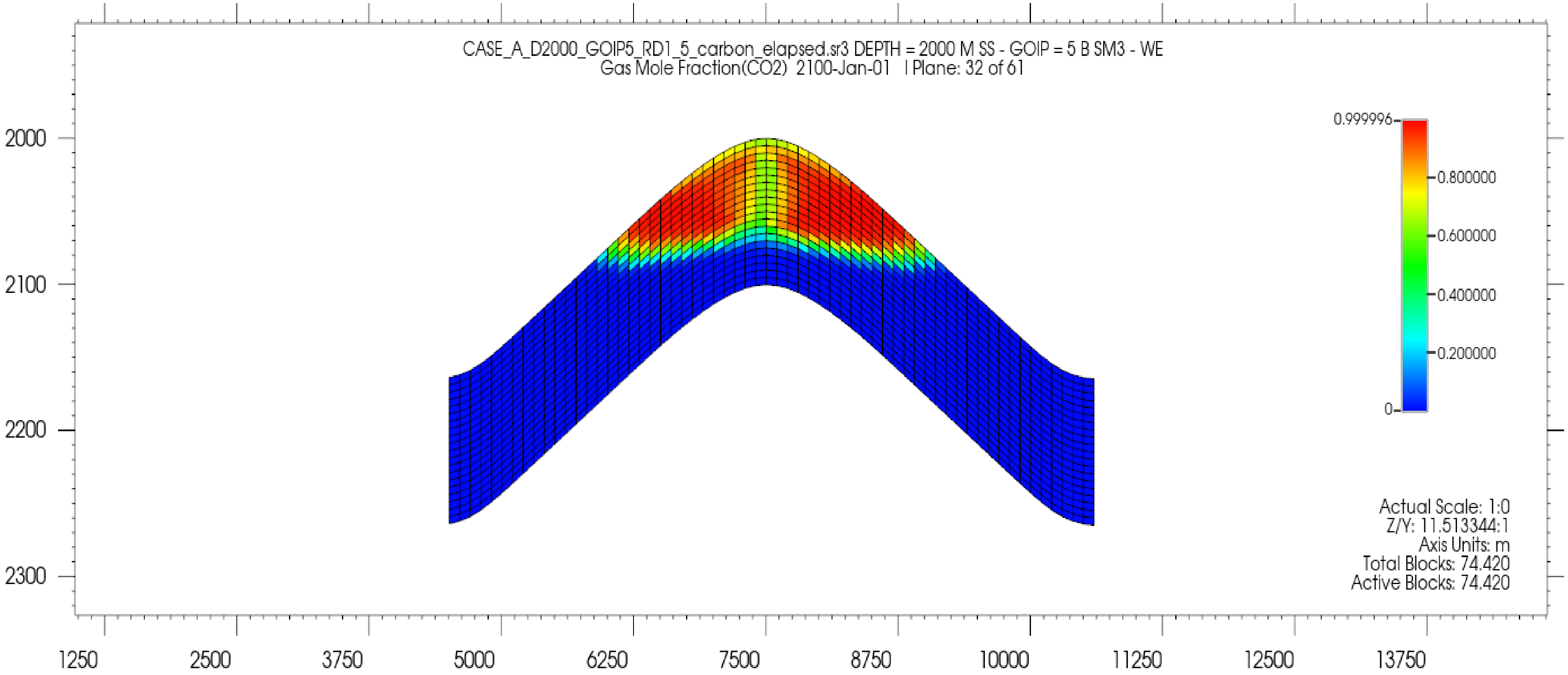

Figure 28 CO_2 injected-case E

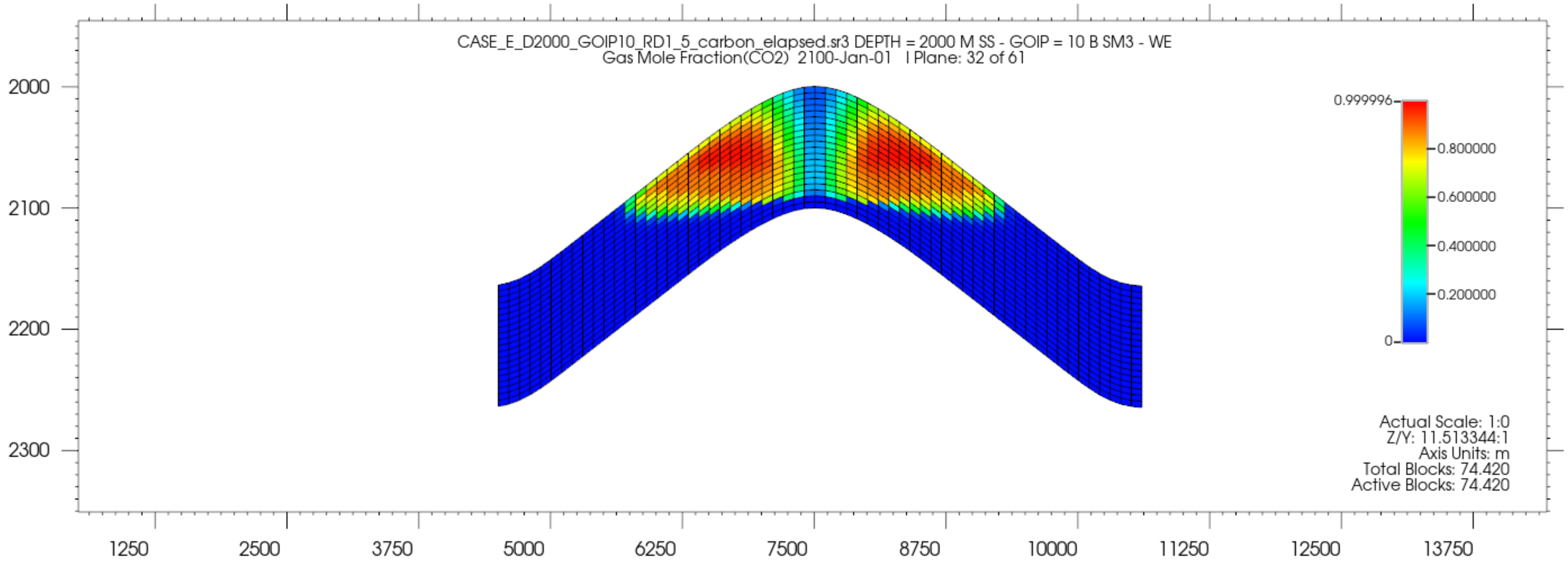

Moreover, the impact of reservoir size on CO_2 injection rates and pressure management is significant. As seen, larger reservoirs generally have a higher capacity to absorb and distribute CO_2, allowing for higher injection rates without causing excessive pressure buildup. This reduces the risk of cap rock fracturing and ensures better containment. Conversely, smaller reservoirs have limited capacity, leading to faster pressure increases and allowing lower rates, thus a longer injection period.

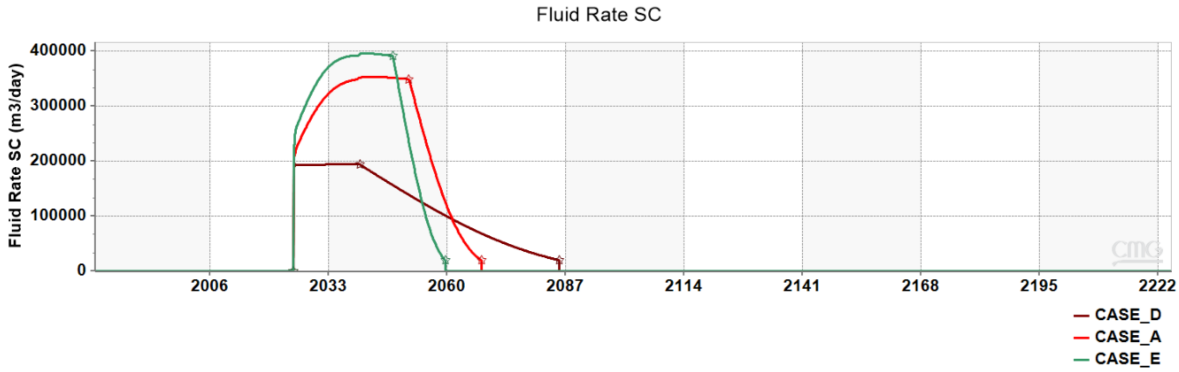

Figure 29 Fluid rate SC- cases D, A, E

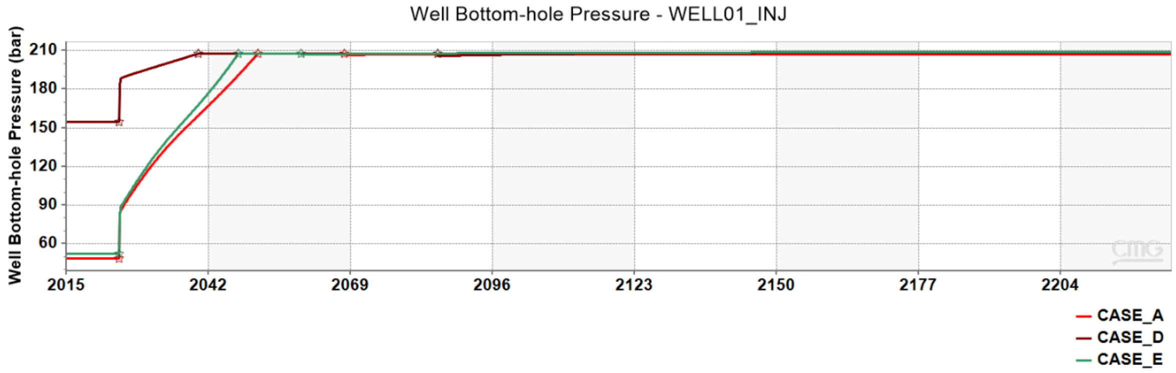

Figure 30 WBHP - cases A, D, E

3. Aquifer size

Discussing aquifers refer to the water influx during the production phase since due to the water drive, the GWC rises after production which leads for sure to a decrease in the storage region of the reservoir, considering as well that the bigger is the aquifer size the bigger is the water influx during the production phase.

To understand the effect of aquifers during injection phases, we will be comparing the models F (rd/re=5) and G (rd/re=10) with the base model A (rd/re=1.5).

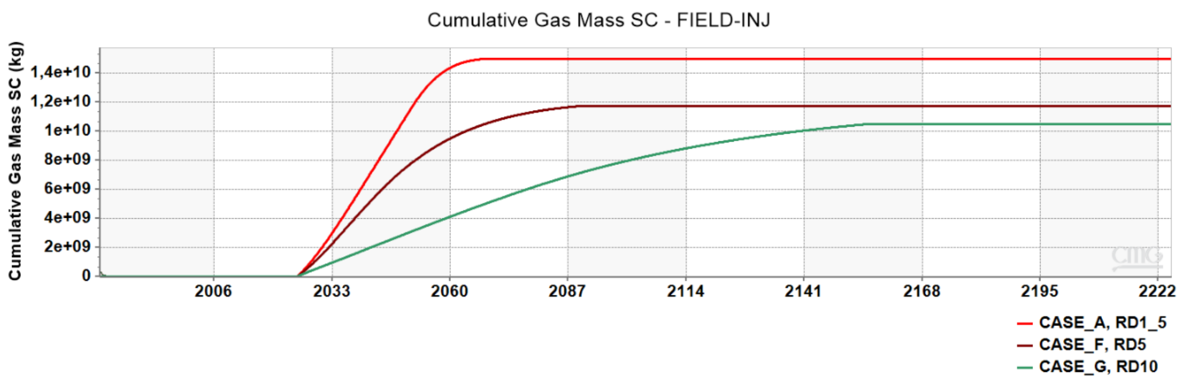

Figure 31 Cumulative CO_2 injected, cases A, F, G

Models	Aquifer size (rd/re)	Total CO2 stored (Kg)	Residual trapping	Solubility trapping	Structural trapping
A	1.5	1.5E+10	35.5 %	6.06 %	58.34 %
F	5	1.2E+10	39.42 %	7.74 %	52.83 %
G	10	1 E+10	40.36 %	8.3 %	51.24 %

Table 12 Amount of CO_2 stored (diff. aqu. size)

The graph clearly indicates that a higher amount of CO_2 is stored in base case A with the smaller aquifer size. To understand these results, the contribution of different trapping mechanisms in the storage will be examined.

When examining the amount of CO_2 trapped by the solubility trapping mechanism, the effect of the solubility of CO_2 becomes clearer and especially in the case of the aquifer with the biggest size due to the high amount of water encroachment. In fact, the highest amount of CO_2 dissolved is in the case G where the water influx was the highest in the production phase due to the big size of the aquifer, thus CO_2 has more amount of water to be dissolved in.

The amount of CO_2 free gas indicates that structural trapping is more important in the base case (smaller aquifer size) and less in the case G with the biggest aquifer size, and this is due to the fact that a bigger part of the CO_2 has been dissolved in case G than in the other models since more water has been entered to the reservoir and thus more pore space has been invaded by water where CO_2 can be dissolved and less possibility for the plume of CO_2 to migrate.

From another point of view, as discussed by Hughes, et al. (2009), CO_2 injection into reservoirs with strong aquifer are likely to present better candidates than the ones with small aquifers since the response of reservoirs with small aquifer is considered more problematic for CO_2 disposal due to the fact that some initial capacity will be compressing up the remaining hydrocarbon gas but after this additional capacity will depend on the rate at which the aquifer will relax in response to the CO_2 injection which may be too low for practical application. However, it is considered by analogy that for reservoirs with strong aquifer, if the water can flow quickly into the pressure sink created by produced hydrocarbon gas, then the water should flow away quickly in response to the pressure spike from the injected CO_2. [23]

And this can be clearer when examining the pressure in the reservoir during injection where the pressure equilibration is better in the presence of an aquifer as compared to the base case, where it tends to increase slightly with time.

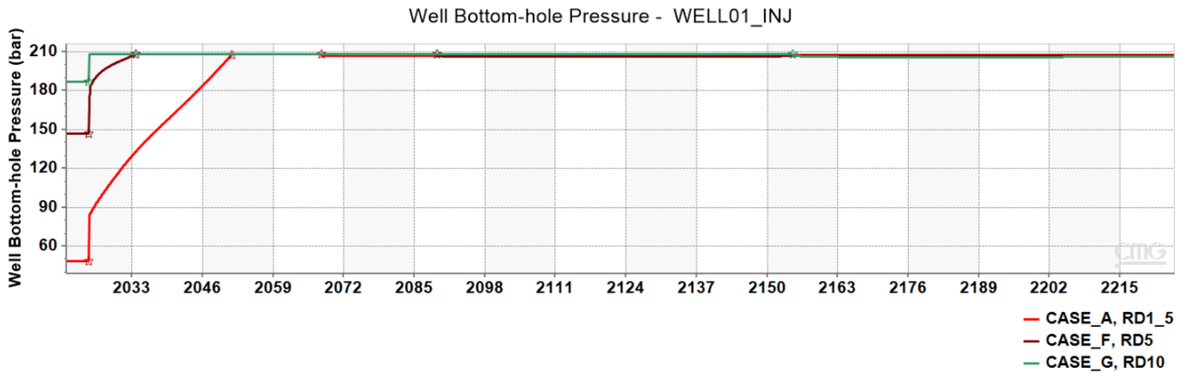

Figure 32 WBHP (diff aquifer size)

Moreover, by injecting CO_2 the water is pushed back, in other words the GWC is pushed down creating additional volume for the CO_2 to be stored. However, not all the previously hydrocarbon-saturated pore space will become available for CO_2 because some residual water may be trapped in the pore space. [19]

4. Porosity

Porosity is one of the major parameters that govern the behavior of the reservoir during CO_2 injection. To understand the impact of porosity, the base model will be compared with two other models, one having a higher porosity of 0.25 and the other a lower porosity of 0.15. In the three models, the same amount of GOIP is considered, thus the GWC was adjusted in each case with different porosity to maintain the same amount of hydrocarbon and perform the comparison.

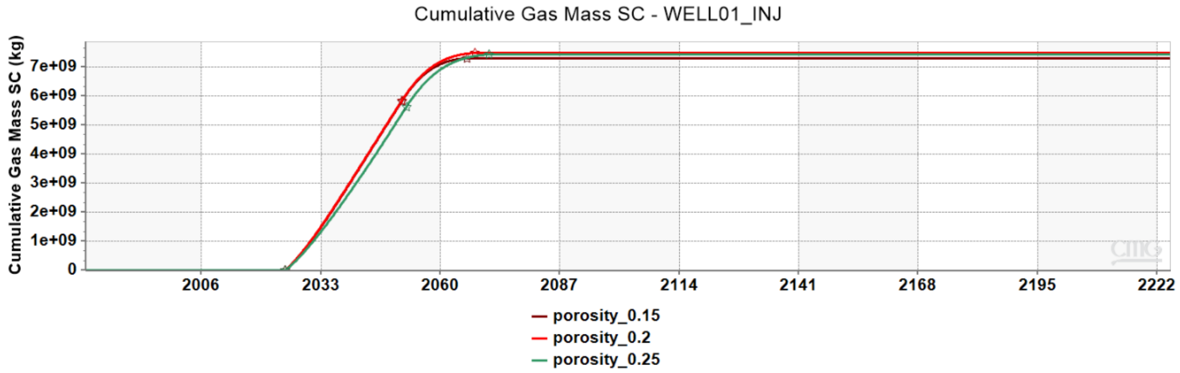

Figure 33 Cum.CO2 captured (diff porosity)

Porosity	**Total CO2 captured (Kg)**	**Residual Trapping (%)**	**Solubility trapping (%)**	**Structural trapping (%)**
0.15	1.5E+10	34 %	5.45 %	60.55 %
0.2 (base case)	1.5E+10	35.5 %	6.06 %	58.34 %
0.25	1.5E+10	36.8 %	6.55%	56.65 %

Table 13 Amount of CO2 trapped by different mechanisms (diff porosity)

The least amount of CO_2 stored is in the case with the lowest porosity which is obvious since with decreasing porosity the available storage space decreases as well leading to less amount of CO_2 stored in the resevoir.

Concerning residual trapping, the results show the higher residual trapping amount in the case of high porosity which is justified for sure by the high amout of pore space and so the highest amount of capillary trapping of CO_2 in the pores. Furthermore, due to the higher pore space, more formation water will be available in the resercoir leading to more amount od CO_2 dissolved.

Moreover, with the increase of porosity we can notice that the amount of CO_2 structurally trapped decrease,which means that the amount of free gas in the reservoir decreases. And this is due to the the extra pore space available which is able to extand the travel time of CO_2 to the caprock and delays its horizontal migration thus affecting the migration of the CO_2 wavefront and decreasing the migation. The figures below show the CO_2 plume migration reduces for higher porosity.

Figure 34 CO2 plume- porosity=0.15

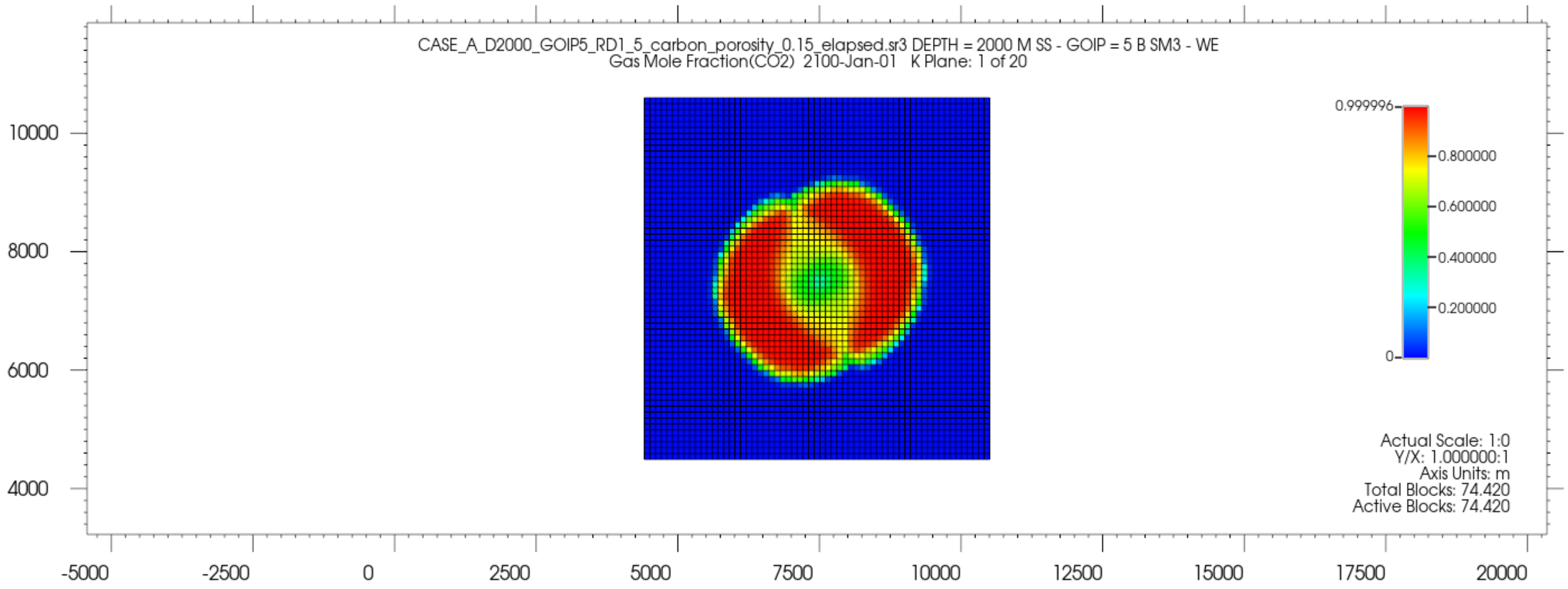

Figure 35 CO2 plume- porosity=0.2(base case)

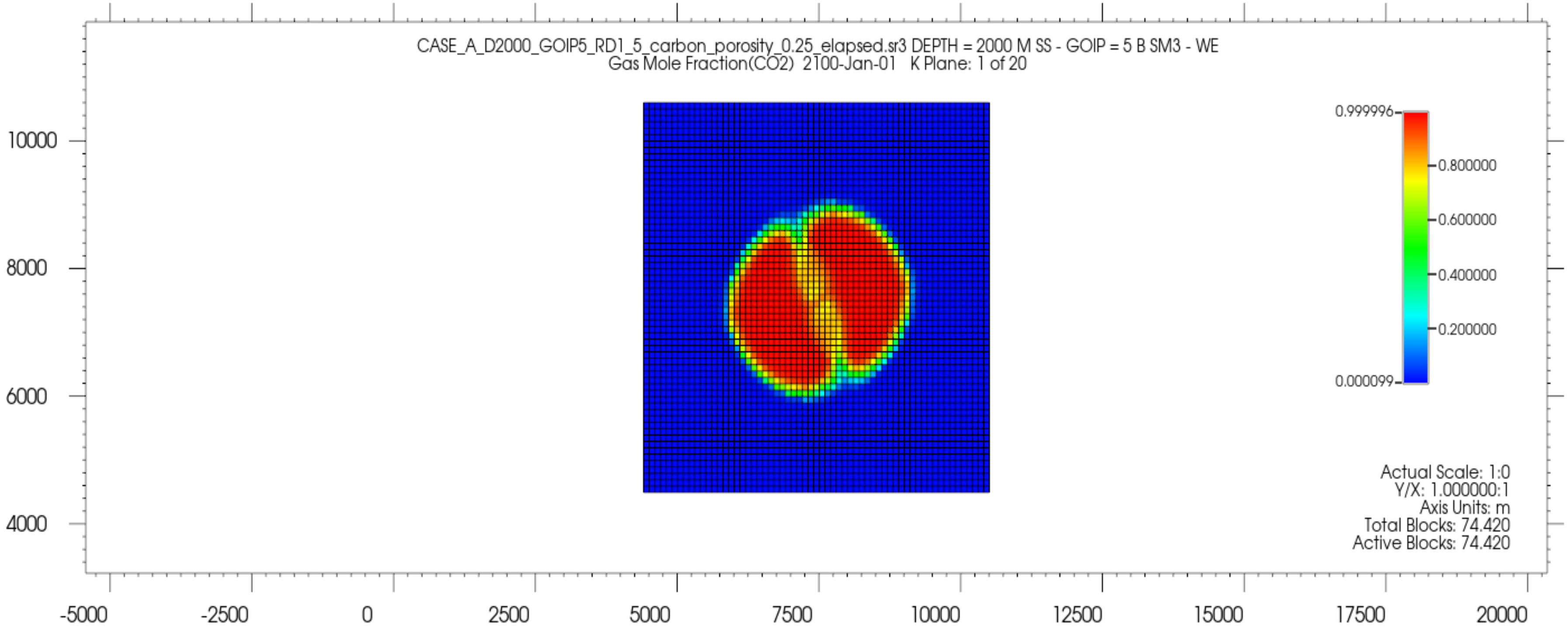

Figure 36 CO2 plume- porosity=0.25

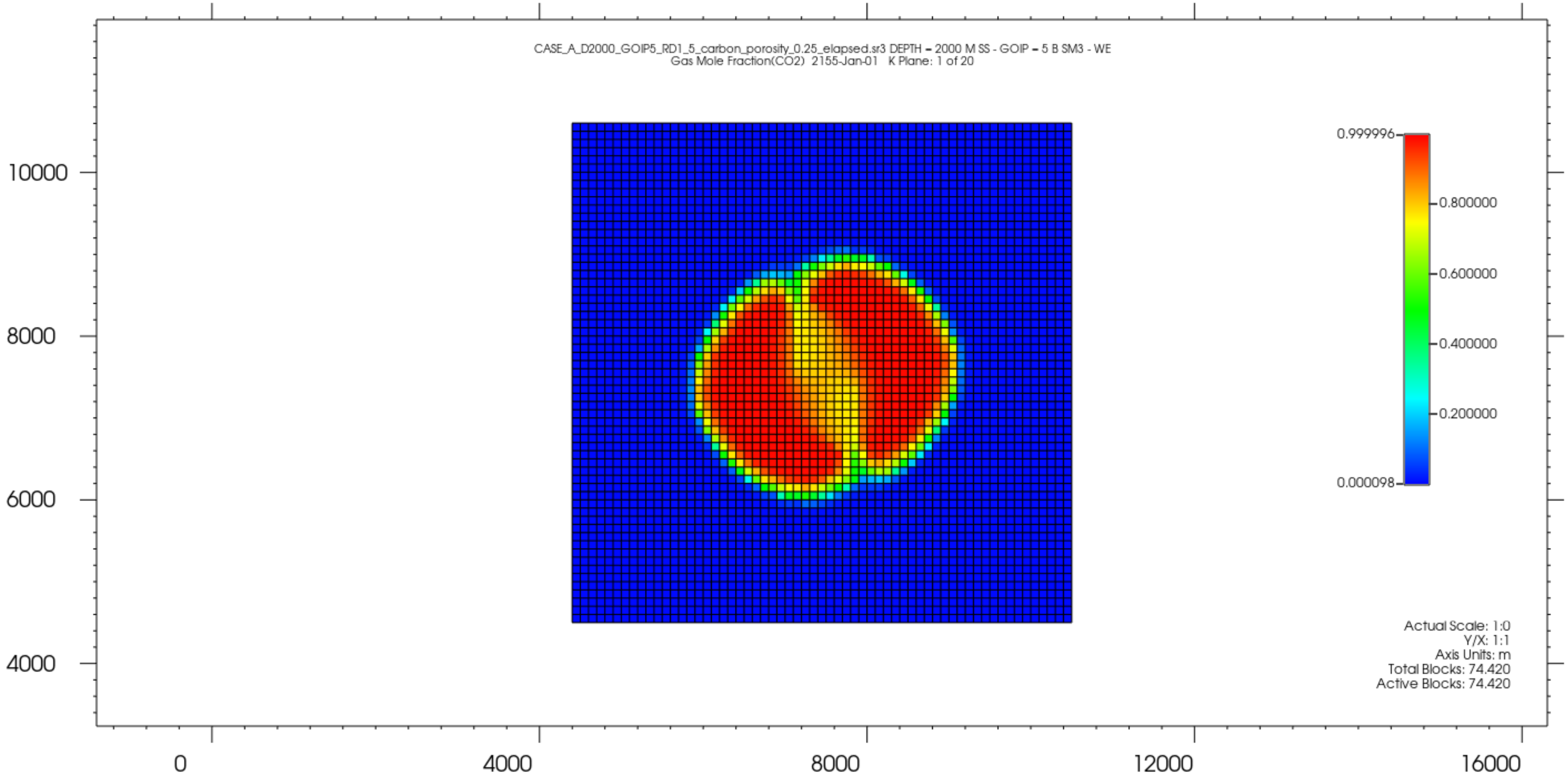

On another hand, the larger the porosity the more amount of CO_2 is needed to be injected to reach the same prerssure and this is clear in the graph showing the pressure profiles, where in the case of low porosity the max BHP constraint is reached before the case of high porosity due to larger pore space. [25]

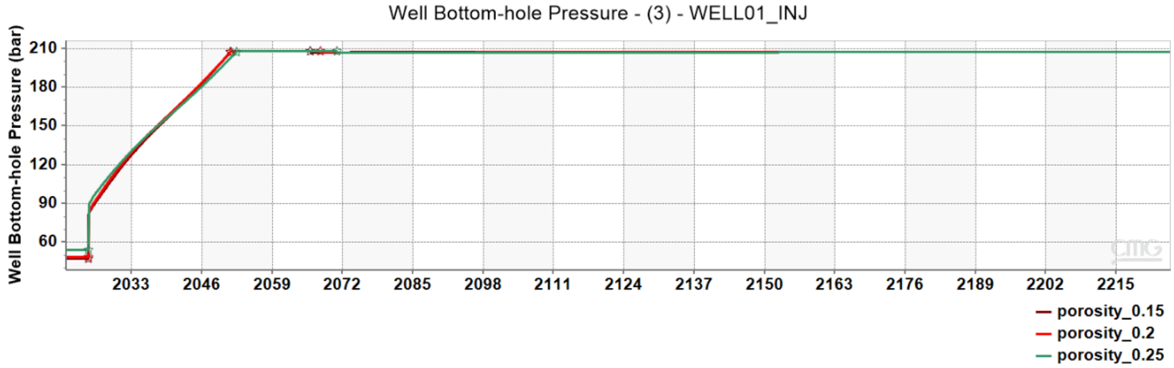

Figure 37 WBHP (diff porosity)

5. Residual gas saturation

The saturation of residual gas in place may affect the CO_2 injection process and reservoir storage capacity. Since gases have higher compressibility and can be efficiently displaced by the injected CO_2, the residual gas saturation tends to give higher storage capacity of a geological porous structure compared to pores filled only with water phase. However, it can have a contrary effect on the fluid flow performance and relative permeability during CO_2 injection. In order to understand the impact of residual gas saturation, the sensitivity will be based on comparing the base model with Sgr=0.2 with a model with lower value of residual gas saturation: Sgr=0.1, and another model with higher value of residual gas: Sgr=0.3.

Sgr	**Total CO2 captured (Kg)**	**Residual Trapping (%)**	**Solubility trapping (%)**	**Structural trapping (%)**
0.1	1.502E+10	18.1 %	6.23 %	75.67 %
0.2	1.5E+10	35.5 %	6.06 %	58.34 %
0.3	1.48E+10	52.9 %	5.9 %	41.2%

Table 14 Amount of CO2 trapped by different mechanisms (diff Sgr)

Starting with the impact of Sgr on the storage capacity, the following graph shows the difference between the cumulative CO_2 stored in the three cases:

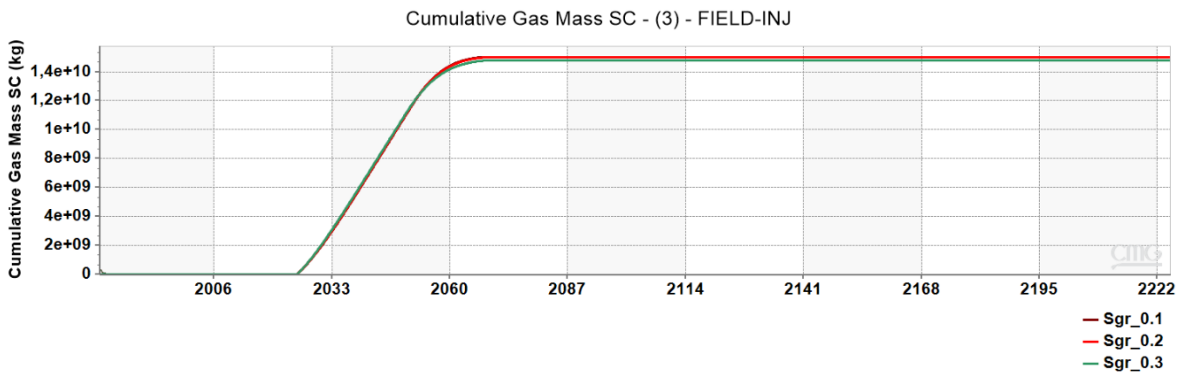

Figure 38 Cumulative CO2 stored (diff Sgr)

The highest amount of CO_2 is stored in the case of the lowest value of residual gas saturation (Sgr=0.1) since residual gas occupies space within the pore network that would otherwise be available for CO_2 storage, thus, higher residual gas saturation means less available pore space for CO_2 injection.

However, from the point of view of trapping mechanisms, the contribution of different mechanisms changes with the value of Sgr.

Residual trapping is one of the mechanisms that is widely affected by residual gas saturation and that is clear by the big differences of the trapped COo_2 between the three cases. The following plot shows this difference more widely:

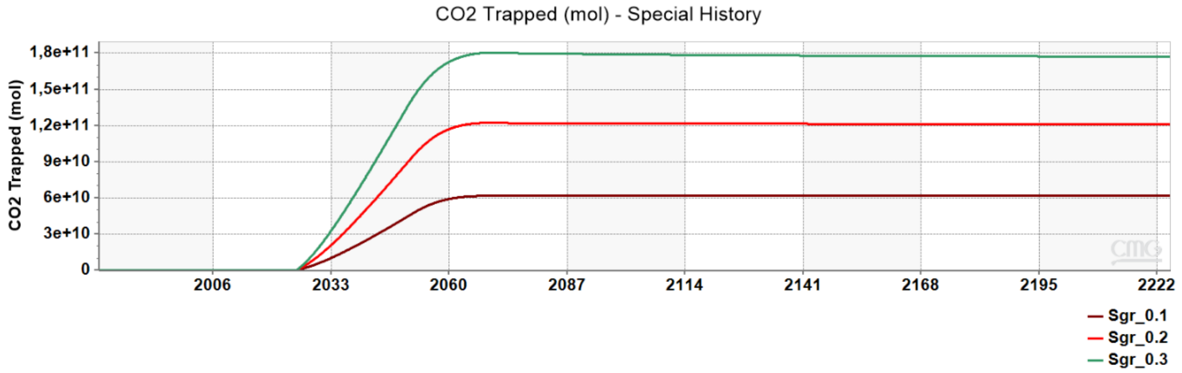

Figure 39 Residual trapping trend (diff Sgr)

The graph explains the direct relationship between Sgr and the amount of CO_2 residual trapped where higher residual gas saturation means that a greater fraction of the CO_2 remains trapped in the pores, enhancing the residual trapping mechanism thus, residual gas saturation can enhance the trapping of CO_2 through residual trapping. CO_2 becomes immobilized as it is trapped in the pore spaces as residual gas, which can be beneficial for ensuring long-term storage security.

From another hand, the Sgr has a direct impact on the flow performance of the CO_2 in the reservoir since it affects directly the relative permeability and this change in relative permeability is clear in the following plots representing the relative permeability curves for the three cases:

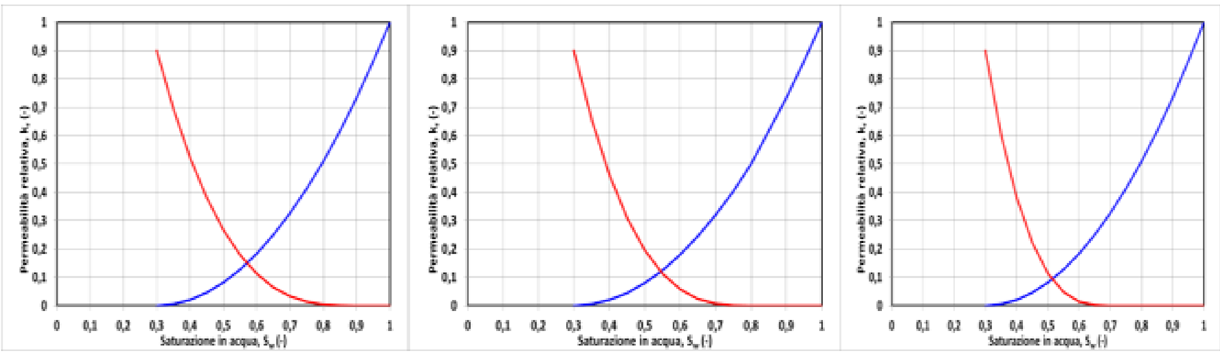

Figure 40 Relative permeability curves according to diff Sgr

The increase of residual saturation leads to a decrease of the relative permeability to gas which leads to a decrease in the migration plume of CO_2. Thus, an increase in the residual gas saturation changes the amount of the structural trapping. It should be noticed from the table values that there is an inverse relationship between the amount of free gas and the remaining gas.

6. Irreducible Water Saturation

Research and studies have shown that that the quantity of CO_2 stored, and its migratory and distribution scopes are very little impacted by the relative permeability of water. Therefore, the focus will be on the effects of the relative permeability of gas (Krg) on CO_2 storage. One important parameter that affects the relative permeability curve of gas is the irreducible water saturation.

For the base case, Swi is equal to 0.3 (30%). The two other simulations run with a reduced value of Swi = 0.1 (10%), and an amplified value with Swi=0.55 (55%).

The following graphs show the relative permeability curves related to gas and water for the 3 models:

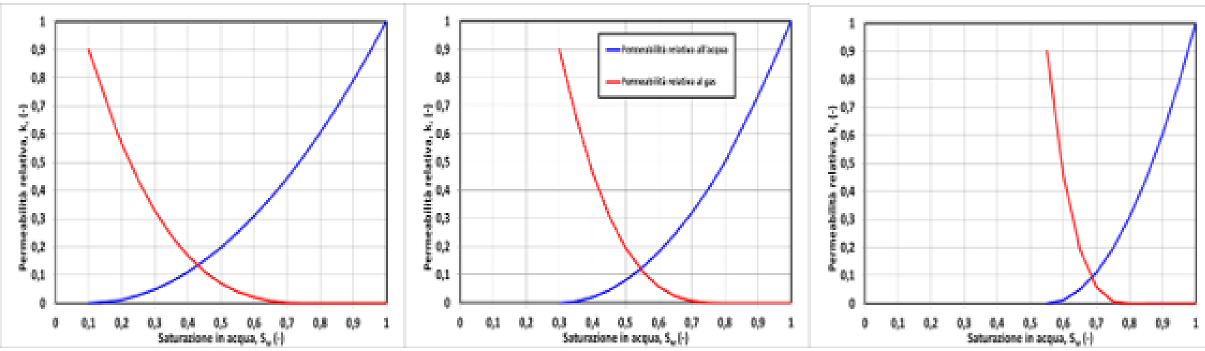

Figure 41 Relative permeability curves according to diff Swi

Swi	**Total CO2 trapped (kg)**	**Residual trapping**	**Solubility trapping**	**Structural trapping**
0.1	1.47E+10	30.72 %	4.41 %	64.87 %
0.3 (base case)	1.5E+10	35.5 %	6.06 %	58.34 %
0.55	1.51E+10	45.75 %	9.6 %	44.65 %

Figure 42 Cum Co2 stored by different mechanisms

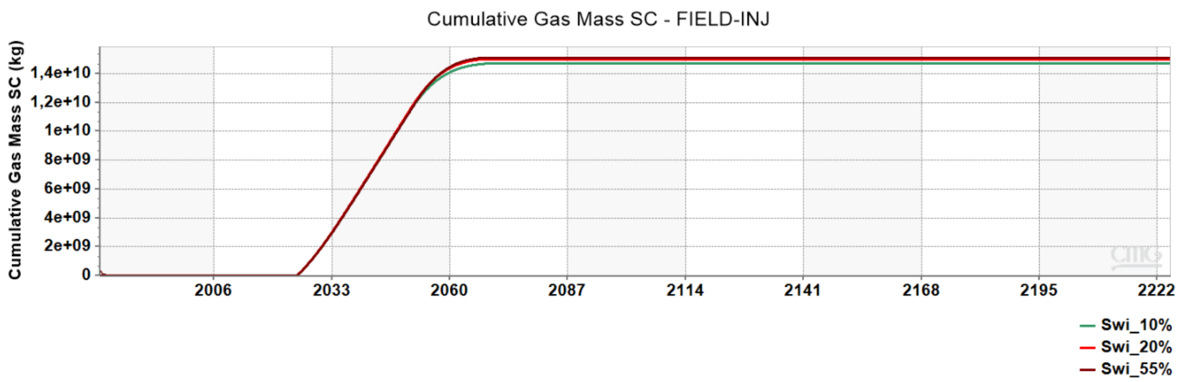

Figure 43 Cum amount of Co2 (diff Swi)

Overall, the highest amount of CO_2 trapped is in the case of the highest value of Swi. In fact, by examining the table representing the different amount of CO_2 trapped by different mechanisms, it can be seen that with the increase of irreducible water saturation the amount of dissolved CO_2 increases, and this can be justified by the increase of the amount of water in the reservoir which led to a higher amount of CO_2 to be dissolved.

The same implies for the residual trapping mechanism, in fact, when Swi increases the amount of CO_2 trapped increases as well. This can be justified by highlighting the differences in the relative permeability curves between the 3 cases, in fact, when the irreducible water saturation increases the relative permeability curve to gas starts getting more vertical, which means that the amount of gas free in the reservoir is reducing since less range of gas is movable with increase of Swi which explains the higher amount of trapped CO_2.

The structural trapping values prove more this point of view by clearly showing the amount of free CO_2 decreasing with increasing the Swi value. Swi affects the migration and buoyancy-driven movement of CO_2. In fact, the low Swi case where most of the gas is extremely mobile CO_2 is trapped mostly structurally since lower Swi allows for more CO_2 to migrate.

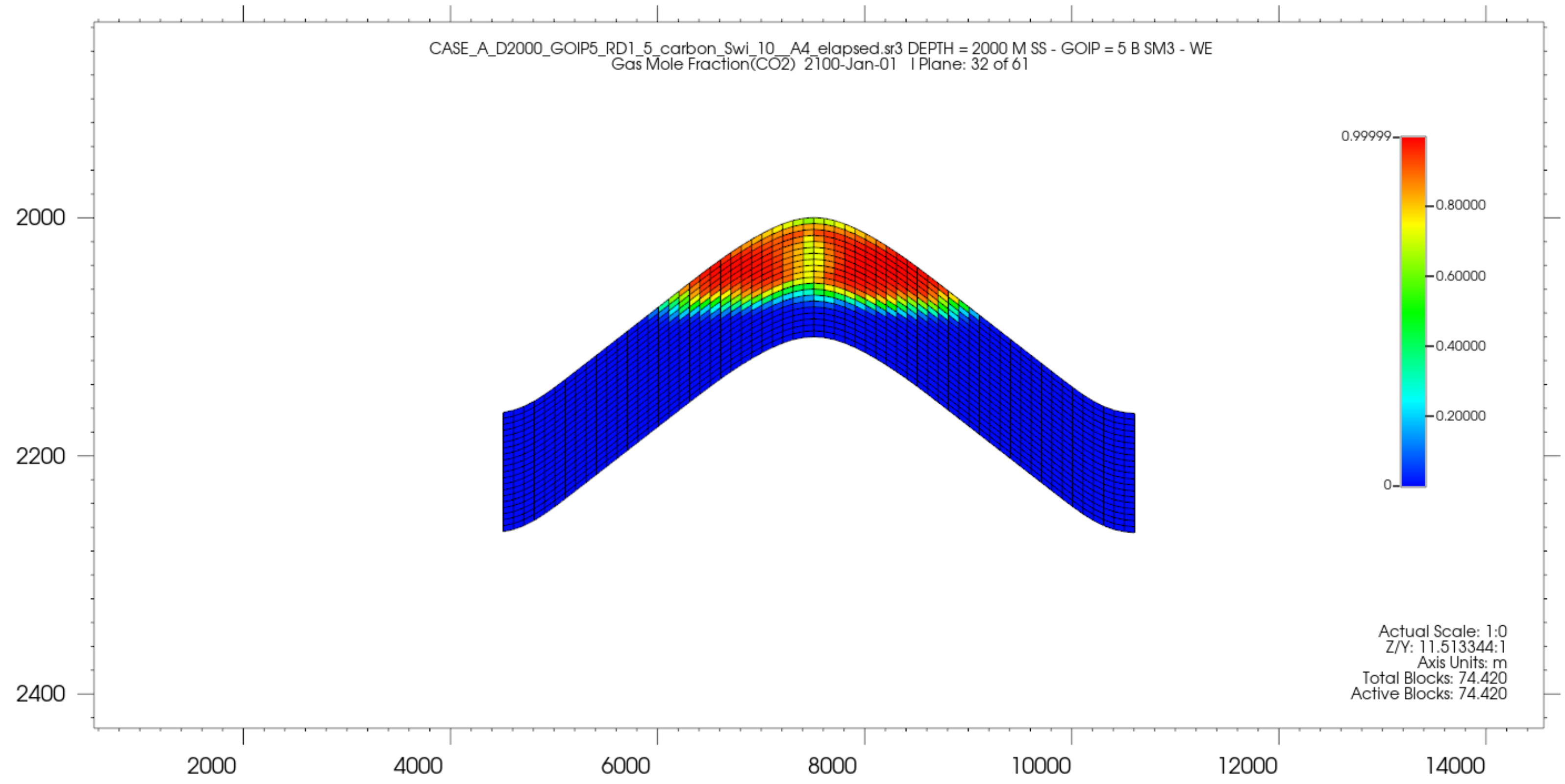

Figure 44 CO2 migration (Swi=0.1)

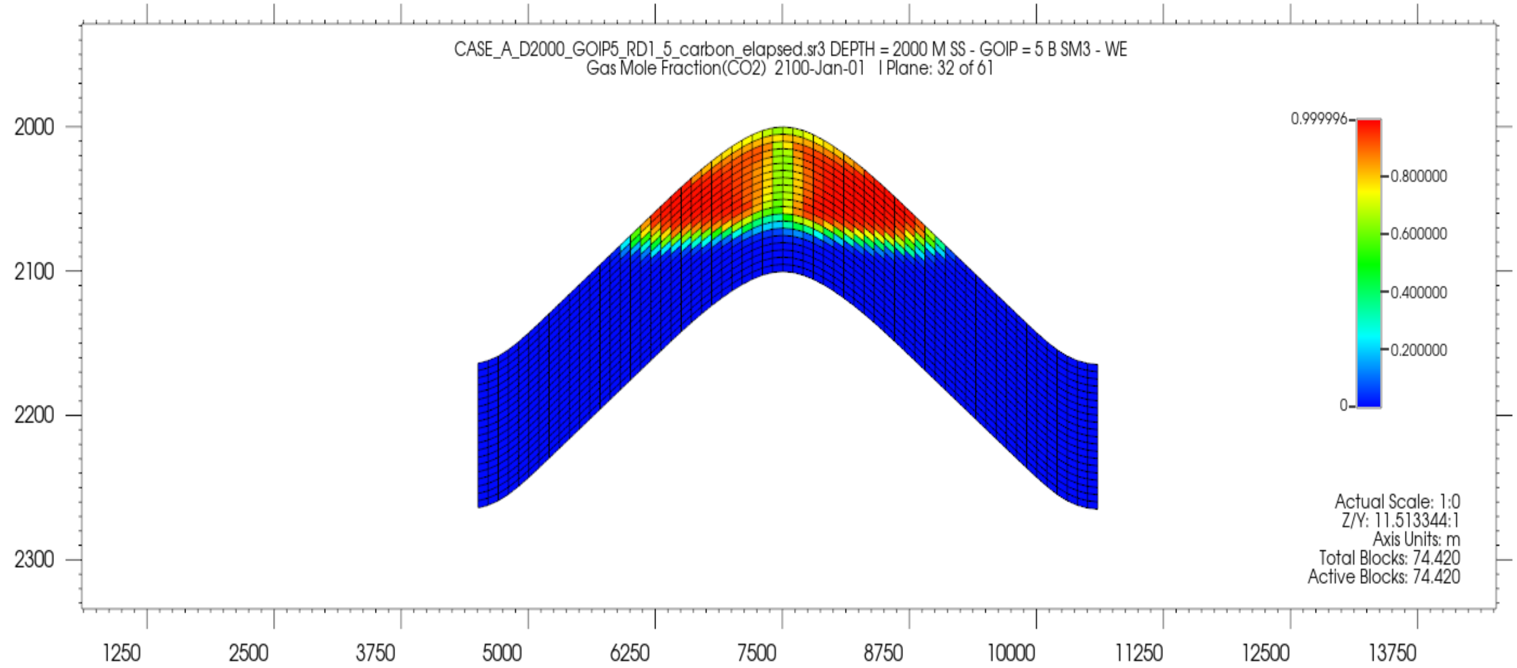

Figure 45 CO2 migration (Swi=0.2)

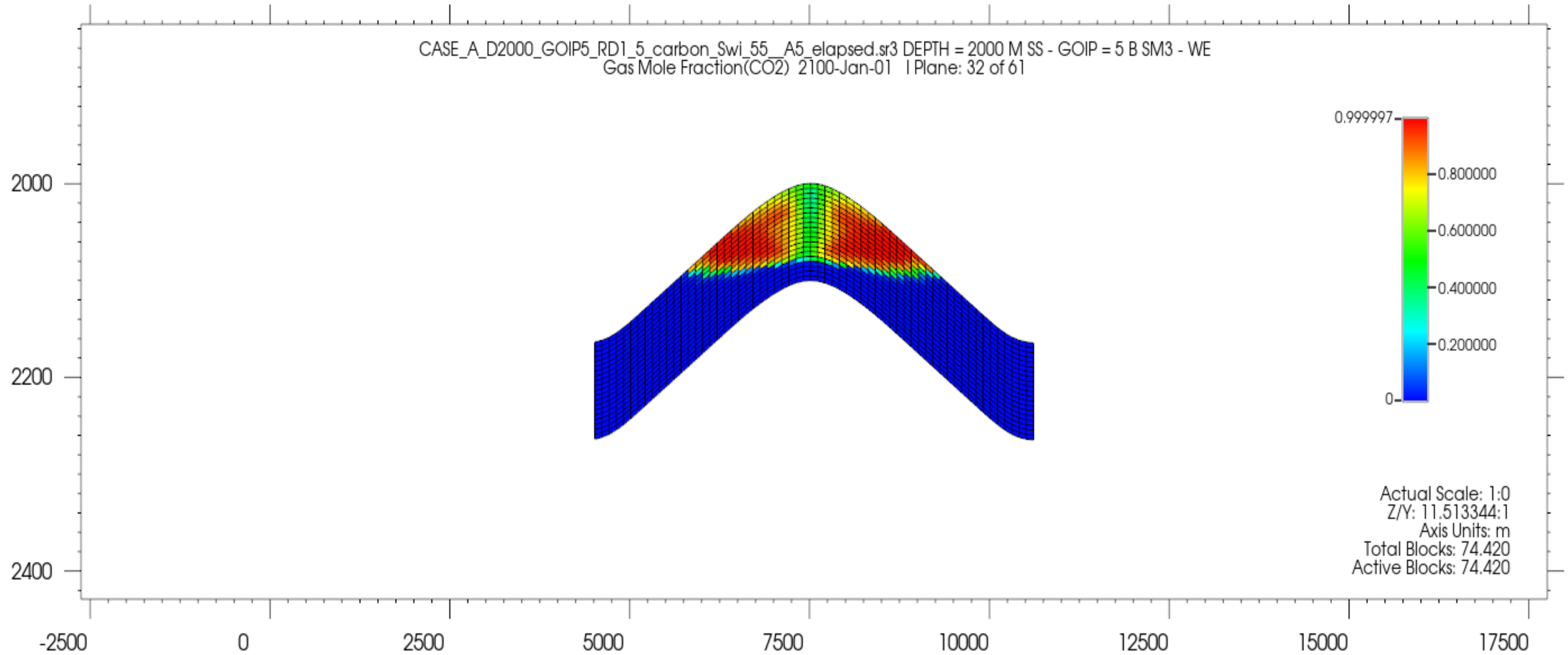

Figure 46 CO2 migration (Swi=0.55)

7. Kr_{CO2} (Swi):

Another parameter affecting the relative permeability curve is the Kr_{CO2} (Swi). In this section a scaling of the end point: Kr_{CO2} (Swi) will be performed to be able to understand more the effect of the relative permeability to gas in CO_2 storage. The following plots show the difference in Krg curves with scaling the end point $Kr_{CO2,\ Swi}$.

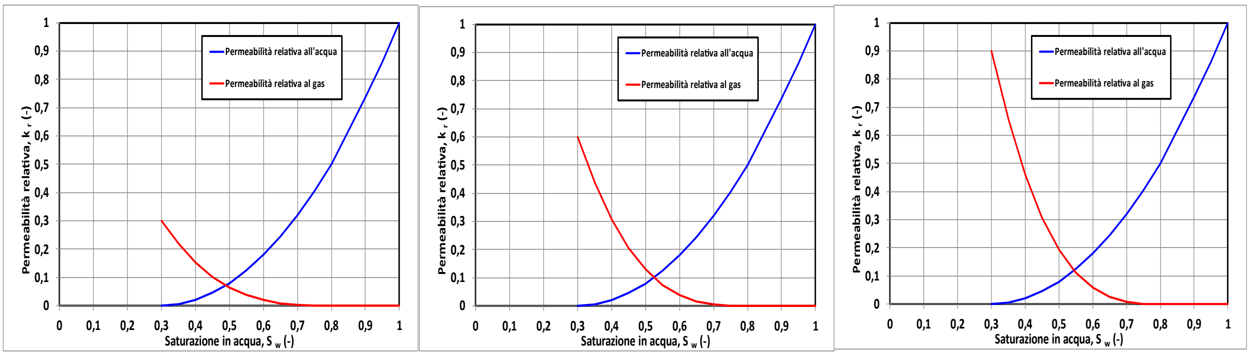

Figure 47 Relative permeabilty curves with scaling of Krco2

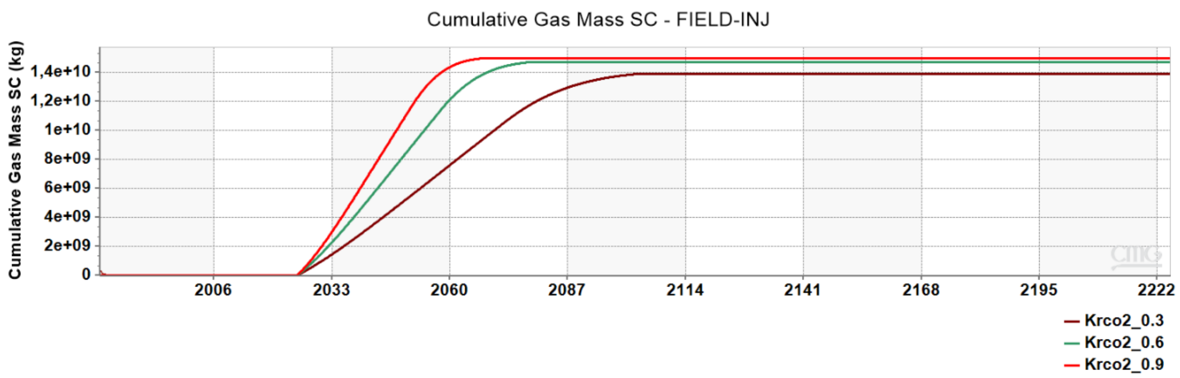

Figure 48 Cumulative CO2 stored (different Krco2)

Kr_co2	**Total CO_2 trapped (kg)**	**Residual trapping**	**Solubility trapping**	**Structural trapping**
0.3	1.40E+10	34.07 %	5.53 %	60.4 %
0.6	1.48E+10	35.01 %	5.84%	59.15 %
0.9 (base case)	1.50E+10	35.5 %	6.06 %	58.34 %

Table 15 Total CO2 trapped & contribution of mechanisms (diff Krco2)

The residual trapping mechanism trend can be justified by examining the relative permeability curves where, by lowering the end point, the curves shift downward, so the relative permeability to gas is small even for high saturations of gas, which means the CO_2 is less movable and more amounts can be trapped which leads to more residual trapping.

In what comes to dissolved gas, it can be interpreted as with the lowering of the end point, thus the relative permeability curves, thus the mobility of the gas less gas will be migrating so less amount of gas will be put in contact with the water which leads to less amount of CO_2 dissolved with lowering the permeability curve end point. However, we can consider that the CO_2 mass dissolved in the water phase is barely affected by changes in the relative permeability curve, varying by less than 0.5% across all models.

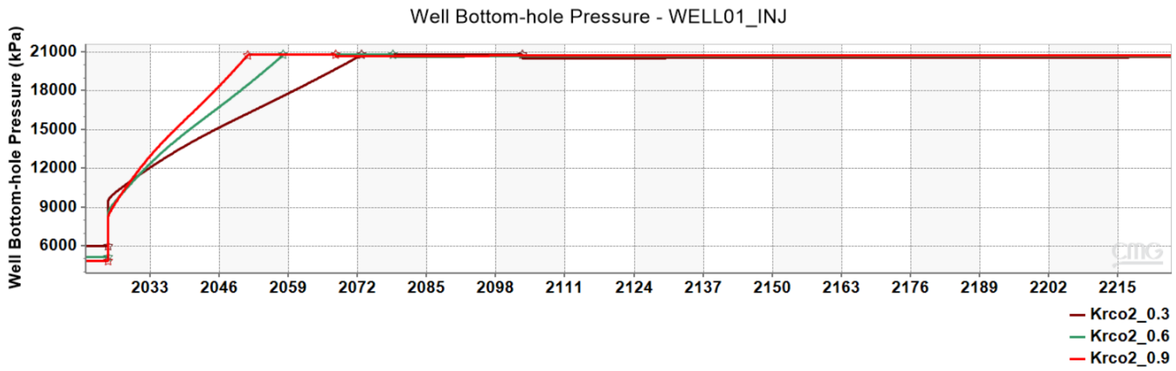

Figure 49 WBHP (diff Krco2)

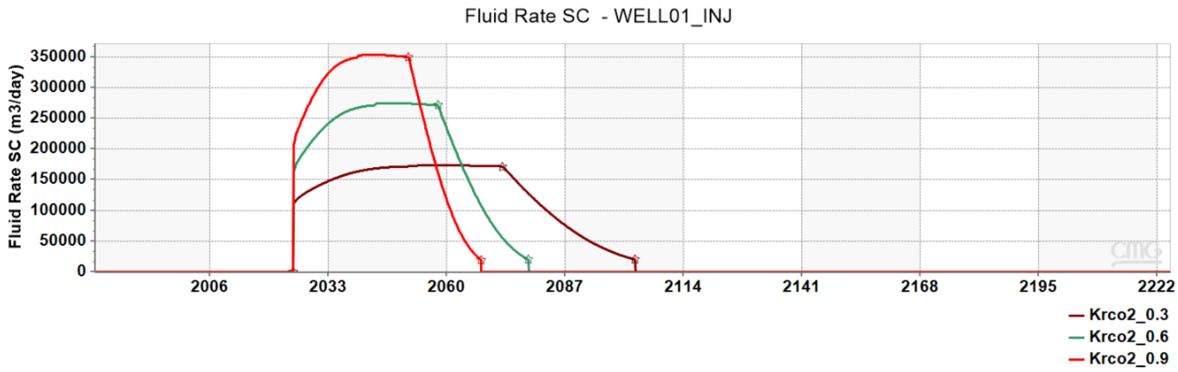

Figure 50 Fluid rate SC (diff Krco2)

Furthermore, Figure 49 indicates how higher permeability facilitates the pressure dissipation in the reservoir since it is clear the rapid increase in the pressure profile for the case of Kr_{co2}(swi)=0.9.

Moreover, higher Kr_{co2} (swi) allows for higher injection rate for CO_2 as shown in Figure 35 since having a higher relative permeability allows CO_2 to be injected without encountering important resistance at high rates, which increases the efficiency of the injection process and achieving the injection in a shorter period.

8. Anisotropy ratio (kv/kh)

Reservoir heterogeneity is an important factor in CO_2 migration, distribution, and storage, and the anisotropy ratio (kv/kh) is an important parameter that reflects the reservoir heterogeneity. [20]

To understand how the anisotropy ratio affects CO2 storage, the sensitivity will be performed by changing the value of the vertical permeability K_v, thus, comparing the base model where k_h =50 mD and k_v= 5 mD, with a model having the ratio 1:10 (k_v=5 mD and k_h=50) and another homogeneous model with k_v=50 mD, k_h =50 mD.

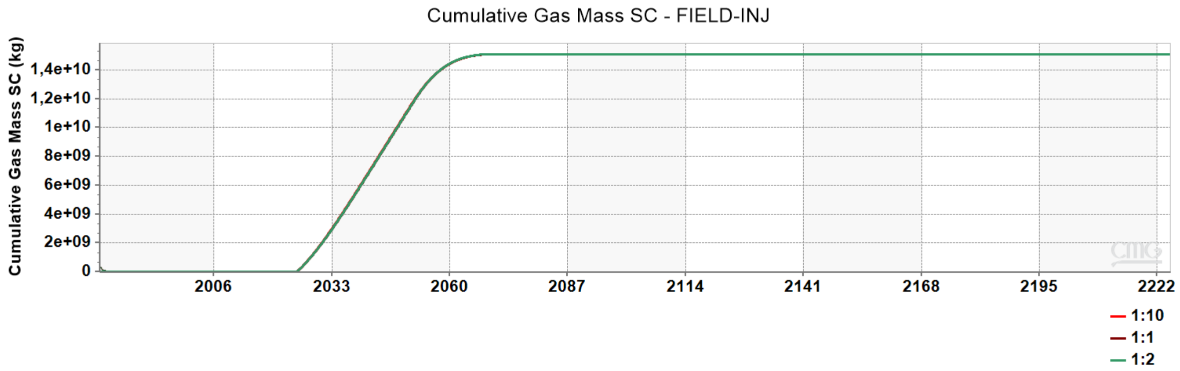

Figure 51 Cum Co2 stored (diff anisotropy ratio)

Kv/kh	**Total CO2 stored (Kg)**	**Residual Trapping (%)**	**Solubility trapping (%)**	**Structural trapping (%)**
1:10 (base case)	1.5E+10	35.5 %	6.06 %	58.34 %
1:2	1.5E+10	35.56 %	6.07 %	58.37 %
1:1	1.5E+10	35.2 %	6 %	58.8 %

Table 16 Total CO_2 stored by different mechanisms (diff. Kv/Kh)

As the results show, the anisotropy ratio does not have an impact on the CO_2 storage capacity and injectivity since for the three cases we got the same total amount of CO_2 stored and the injection was done during the same time, so no effect on injectivity as well.

9. Absolute permeability

In this part, the influence of the absolute permeability on CO_2 storage is being investigated by comparing the base model with an absolute permeability of 50 mD with two different models having an absolute permeability of 20 mD and 50mD respectively.

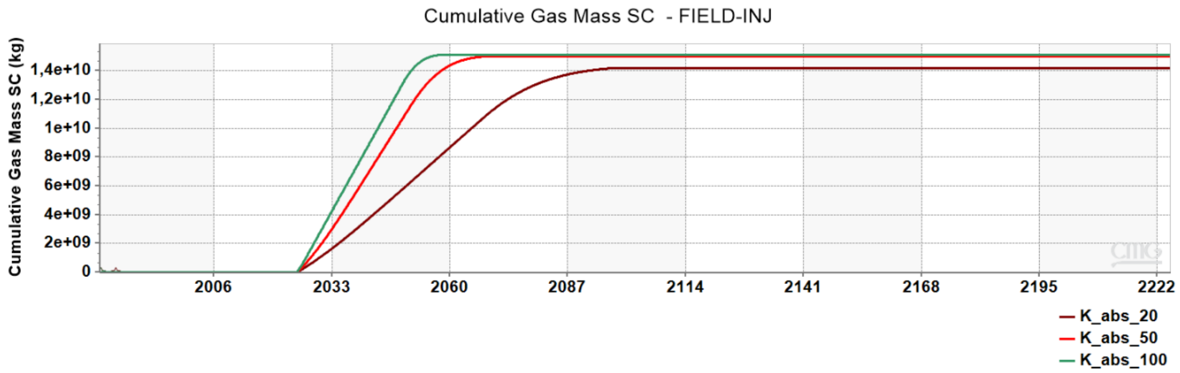

Figure 52 Cum CO2 stored (diff Kabs)

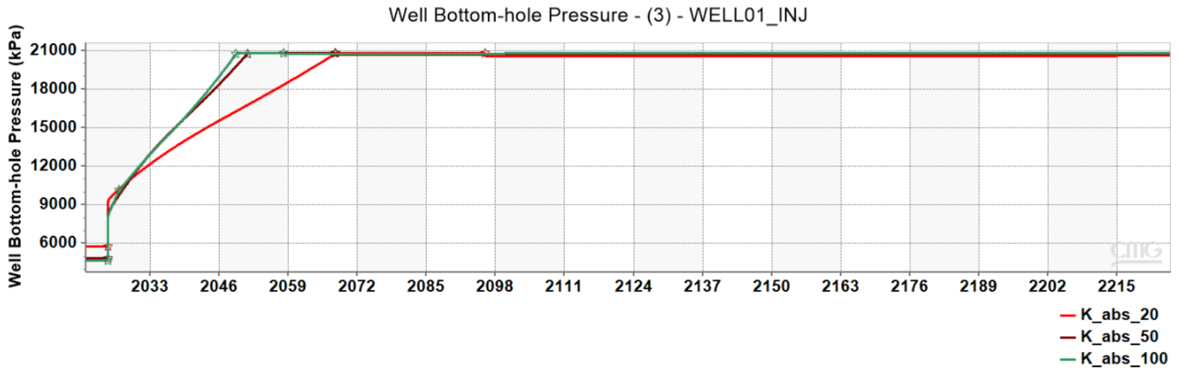

Figure 53 WBHP (diff Kabs)

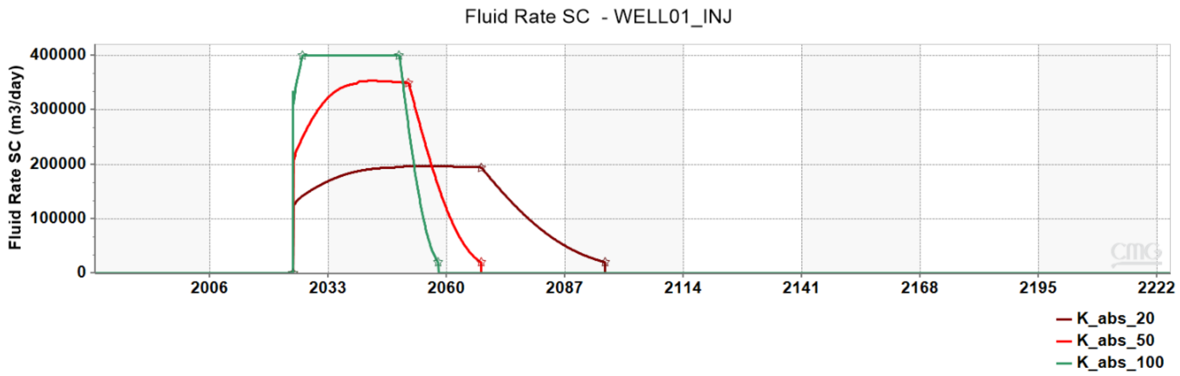

Figure 54 Injection rate (diff Kabs)

Kabs	**Total CO2 stored (Kg)**	**Residual Trapping (%)**	**Solubility trapping (%)**	**Structural trapping (%)**
20 mD	1.4E+10	35.2 %	5.9 %	58.9 %
50 mD	1.5E+10	35.5 %	6.06 %	58.34 %
100 mD	1.52E+10	35.57 %	6.07 %	58.36 %

Table 17 Total CO2 stored and contribution of mechanisms (diff Kabs)

As the results show there is no big difference in the total CO_2 stored in the three different cases, mentioning that the amount of CO_2 in the case of higher permeability is a bit larger than the other cases due to better connectivity between pore spaces. However, an important difference is clear regarding the time needed for injection between the three different cases as well as between the pressure profiles.

As evidenced in the graph, injectivity depends strongly on the reservoir permeability. Due to high permeability, the CO_2 migrates faster in the reservoir allowing higher injection rate since the formation offers less resistance to the CO_2 flow in the reservoir, thus a faster injection which helps reduce the injection period. However, in the case of low permeability, lower injection rates are required to prevent excessive pressure build up.

In fact, the max well bottom hole pressure is reached first as well in the case of the higher permeability since higher absolute permeability allows faster and better pressure dissipation in the reservoir. Moreover, the build-up pressure is the highest in the case of lowest reservoir permeability.

10.Injection rates

The injection rate in the context of CO_2 storage is a critical parameter that influences enormously the effectiveness, safety, and economic viability of storage projects; thus, it is an important parameter to determine the injectivity and efficiency of a long-term storage. To achieve an optimal injection rate, a balance between different factors is required as pressure management, environmental considerations…. High injection rates can be considered efficient for the aim of meeting the net zero goal, however they may lead to high chances of geo-mechanical fractures. While a very low rate may limit the efficiency of CO_2 storage and prolong storage timeline

Model A has not been used in this sensitivity since as mentioned previously, no constant rate was imposed in the simulations, however the rate was a consequence of the constraint specified by the difference of pressure between the Head and Bottom well. For this case, sensitivities will be performed on three different injection rates to understand the effect of each rate and the CO_2 storage performance in each case. The base case will be considered with a constant injection rate of 300 M m3/day and compared with a case of 200 M m3/day and another of 400 M m3/day, considering that in each case two injection wells are operating. The same properties and reservoir characteristics already specified previously for model A are defined in these simulations as well.

Rate (M m3/day)	Total CO2 stored (Kg)	Residual Trapping (%)	Solubility trapping (%)	Structural trapping (%)
200	1.5E+10	35.47 %	6.01 %	58.5 %
300	1.5E+10	35.69 %	6.10 %	58.2 %
400	1.5E+10	35.7 %	6.10 %	58.2 %

Table 18 Total CO_2 stored and contribution of trapping mechanisms (diff rates)

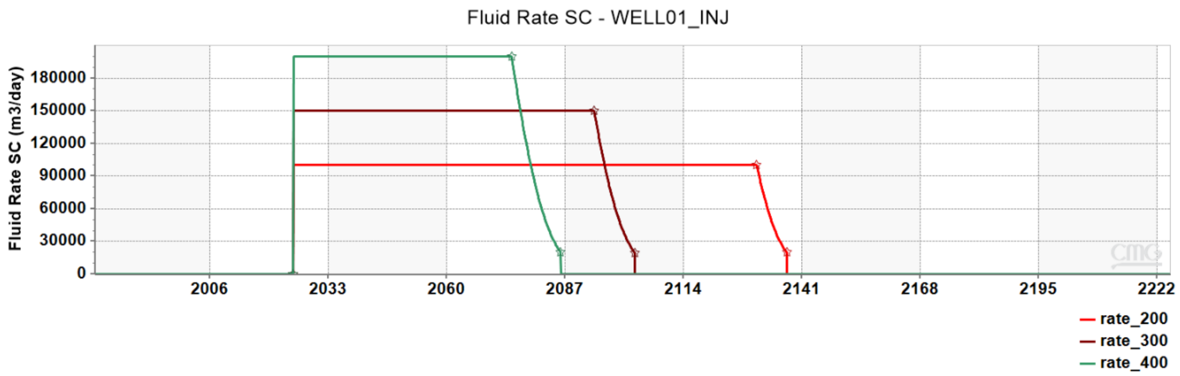

Figure 55 CO2 injection rates sc

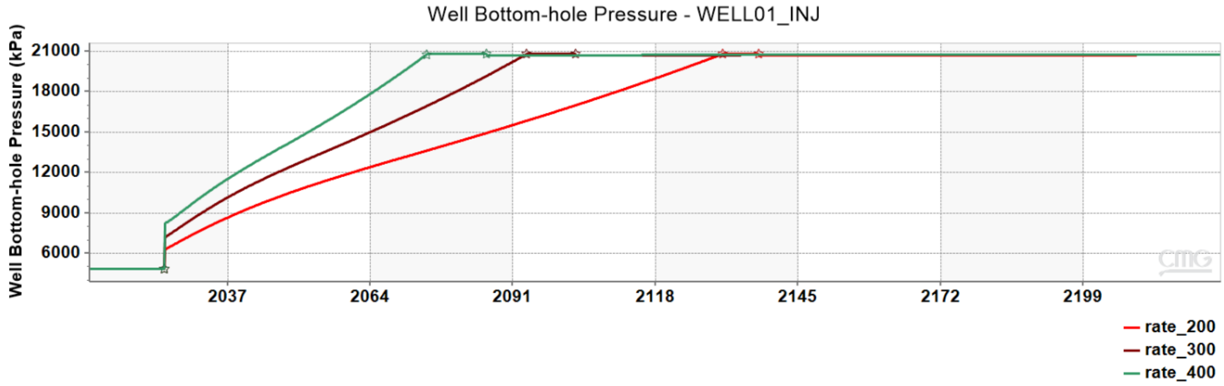

Figure 56 WBHP (diff rate)

First, as seen in the table, the model simulating the highest rate (400Mm3/day) has the highest amount of CO_2 stored after injection, thus, with a higher injection rate the total amount of CO_2 stored increased. Moreover, it's crucial to note that this amount of CO_2 is the highest even after 100 years, which means in the case of the highest rate, no leakage of CO_2 has occurred during the years post-injection thus this high rate didn't reach the fracture limits of the reservoir and did not cause any leakage pathway for the CO_2.

Furthermore, with the high rate the CO_2 injection period is the shortest. In fact, the relationship between injection rate and pressure is clearly a direct correlation: the increase in the rate of injection, and consequently the total amount of fluid injected, causes a linear increase in pressure. As shown in Figure, the higher the CO_2 injection rate, the greater the reservoir pressure, thus the max BHP constraint has been violated first in the case of a rate of 400 Mm3/day.

In order to be able to compare more the efficiency and the better injectivity between the three models, the injectivity index will be calculated. Noting that the injectivity index was not calculated in the previous sensitivities since no constant rate was imposed during the injection scenarios.

The injectivity index is a measure of the well fluid take at a given WHP or reservoir pressure. It is normally measured in tonne/h/bar or kg/s/kPa or kg/s/bar… [29]

$$I = \frac{Q_{inj}}{\Delta P}$$

with $\Delta P = P_{wf} - P_i$

We are calculating the three indexes at the same date - 01/01/2060, to be able to compare:

Rate (M m3/day)	**Initial Pressure (bar)**	**Pwf (1/1/2060) (bar)**	**Injectivity index (Mm3/day/bar)**
200	48.528	118.53	2.86
300	48.528	142.25	3.2
400	48.528	167.261	3.37

Table 19 Injectivity index calculations

These results highlight more the increase of injectivity and efficiency of CO_2 storage with a high rate. However, in these cases the fracture limits of the reservoirs should be taken into consideration since high injection rates can cause rapid pressure build-up in the reservoir which can increase the risk of fracturing the caprock, leading to potential CO_2 leakage.

11.Ramp-Up injection strategy

A ramp-up injection strategy is an approach consisting in injecting CO_2 into geological formations where the injection rate gradually increases over time. This strategy is implemented to manage reservoir pressure and ensure the integrity of the reservoir. It involves starting at a low injection rate and progressively increasing it, allowing for continuous monitoring and adjustment based on reservoir response. In the following, the study will be based on investigating the impact of the number of steps considered in a ramp-up injection strategy and its influence on the injectivity of the wells.

In the following analysis the ramp-up injection strategy has 2 wells operating in each model starting on 1/1/2025, first model consists of two-time steps strategy: first 5 years with a rate of 150 000 m^3/day (thus 75 000 m^3/day per well) and then increased for the later years for 300 000 m^3/day (or 150 000 m^3/day per well). Second model consists of four-time steps strategy as follows (per well): first 3 steps are 20 months long and each well is operating with a rate of 37 500 m^3/day, 75 000 m^3/day, 112 500 m^3/day respectively for each step, and the last step starting on 1/1/2030 with the max rate 150 000 m^3/day per well. The following plots highlight the injection rates and steps.

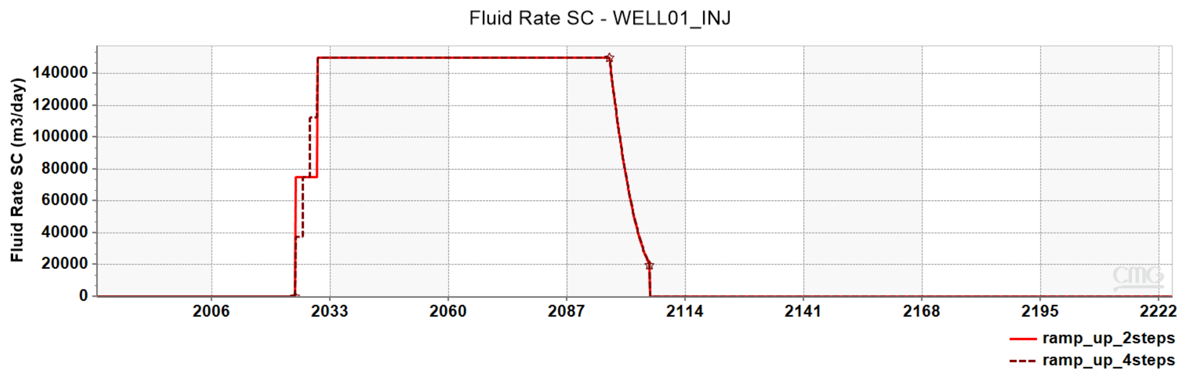

Figure 57 Ramp-Up injection rates: 2 and 4 steps (well 1)

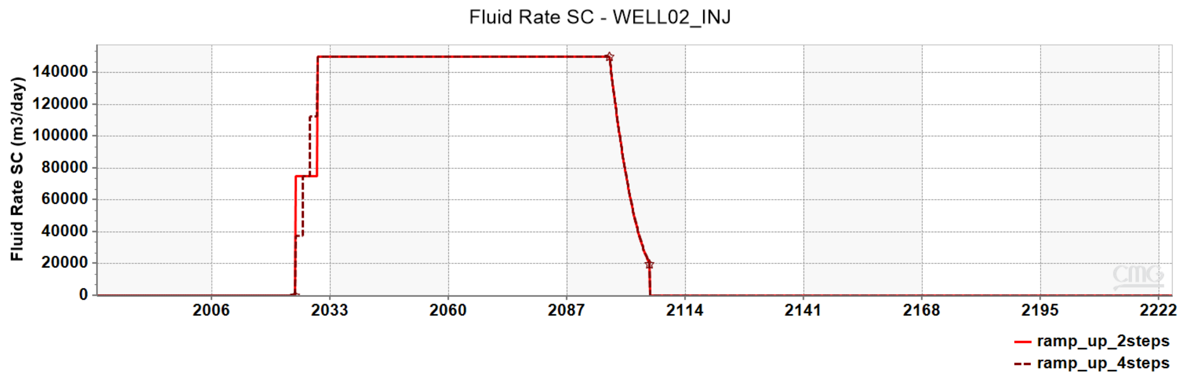

Figure 58 Ramp-Up injection rates: 2 and 4 steps (well 2)

Ramp up	**Total CO2 stored (Kg)**	**Residual trapping (%)**	**Solubility trapping (%)**	**Structural trapping (%)**
2 steps	1.5E+10	35.13 %	7.6 %	57.27 %
4 steps	1.5E+10	35.13 %	7.6 %	57.27%

Table 20 CO2 stored (ramp up)

Concerning the storage amount of CO_2, the results show that in both cases the trapping mechanisms are playing same role and contributing the same in both injection strategies, which concludes that the number of steps in a ramp up injection strategy does not influence the efficiency of the trapping mechanisms in a CO_2 storage process.

On another hand, the results show a difference in the trend of the cumulative CO_2 mass between the years 2025 and 2030 which refer to the years where the rate is being increased. In fact, in the case of 2-steps strategy, the injection is starting with a rate (150 000 m^3/day) higher than the ones initialising the 4 steps strategy (37 500 m^3/day, 75 000 m^3/day and 112 500 m^3/day) thus, in the first case with higher rate, the trend is a bit higher than the case of 4-steps strategy but, in 2030 both operate at the same rate, consequently same trend.

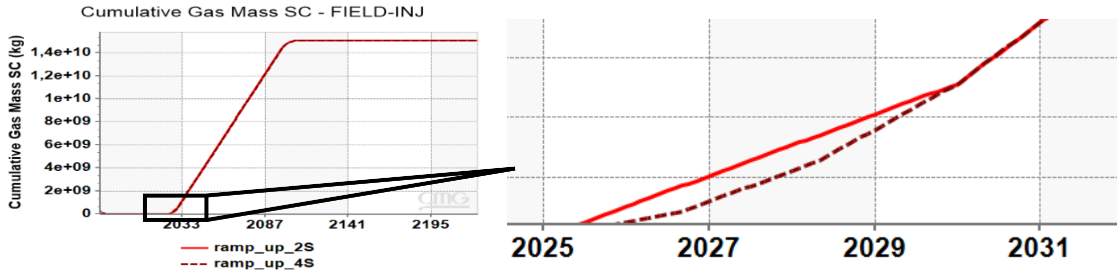

Figure 59 Cum CO2 stored (different injection strategy)

Furthermore, the influence of the difference in rates between the years 2025 and 2030 can be visible in the pressure profile as well, and it leads to a faster pressure trend in the first case.

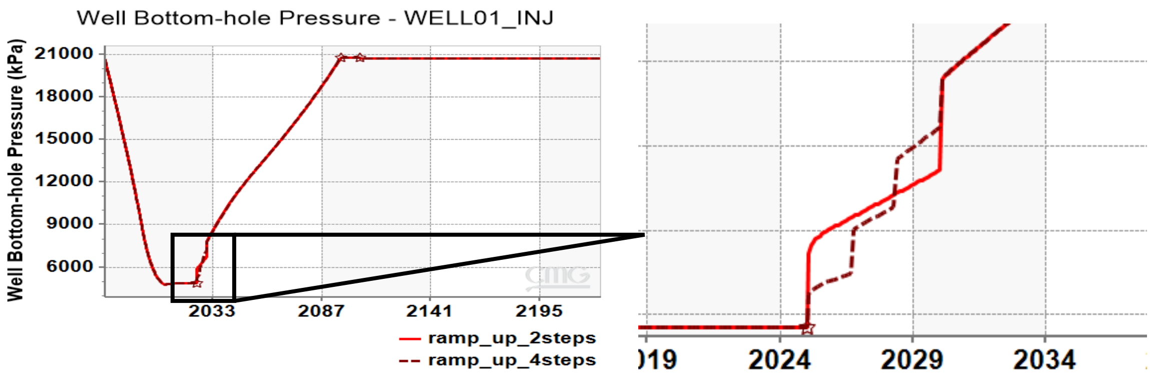

Figure 60 WBHP (different injection strategy)

Consequently, one can conclude that lower injection rates lead to a more controlled increase in reservoir pressure and the fast WBHP increase can be avoided which help in reducing the risks associated with overpressure and can help in maintain the structural integrity of the wells.

VI. Comparison & Discussion

In the following a comparison between the cases covering the storage capacity and the injectivity will be performed to summarize the different impact of the parameters considered in a CO_2 storage process.

1. Storage Capacity

In the following chart, the total amount of CO_2 stored in the year 2155 will be compared for each sensitivity between the two most distinct values of the parameters already investigated. Taking into consideration that the sensitivities related to the ramp up injection strategies and rates differences are not considered in this part since they affect the injectivity and injection strategy of the reservoir, not the storage capacity.

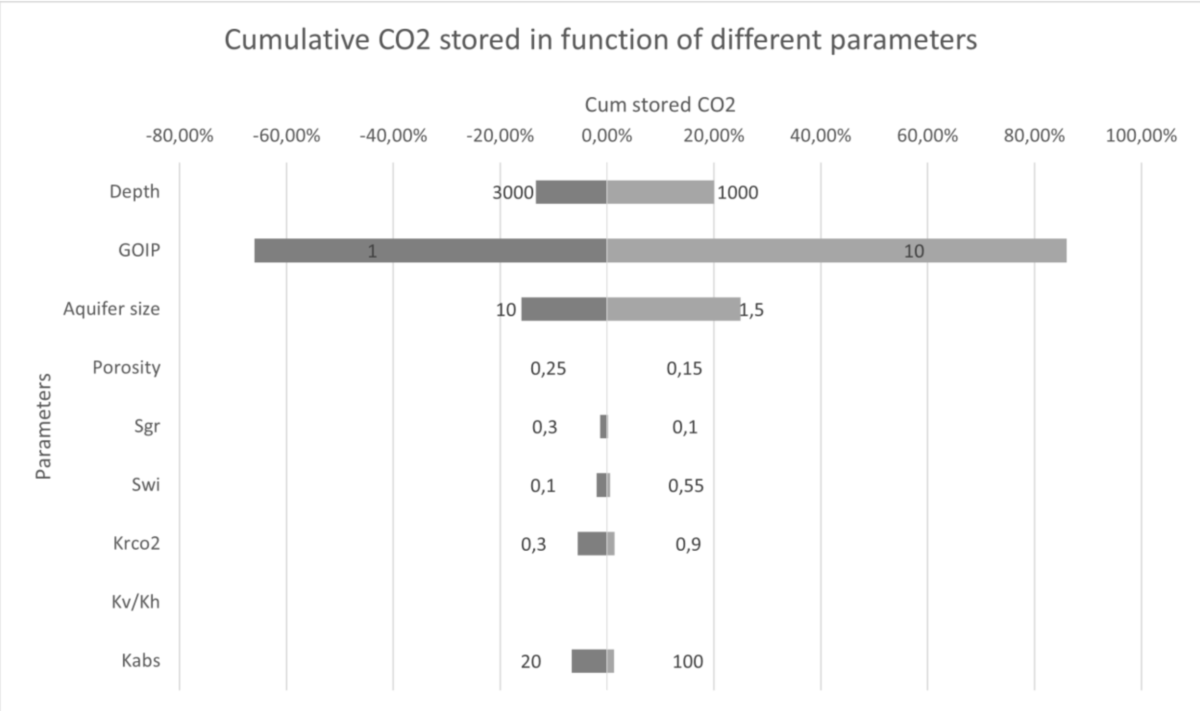

Figure 61 Effect of investigated parameters on the CO2 storage capacity

It is obvious that the parameter that is most affecting the storage capacity is the GOIP, in other words the reservoir size, which is logical since the reservoir size is the first factor related to the capacity determining the available space underground.

Then aquifer size is playing an important role as well, however it is inverse to the GOIP effect since with the increase of the aquifer size, the storage capacity decreases.

Similar to the effect of aquifer size, the depth can have an important effect, inversely proportional to the storage capacity as well. This was discussed mainly by investigating the impact of depth on the CO_2 properties.

The other parameters have also an influence on the storage capacity, smaller than the previously mentioned but still their effect is considerable relatively.

In fact, absolute permeability has shown an effect on the cumulative stored capacity of CO_2 which highlights its importance to take it into account.

This implies as well to the residual gas saturation, irreducible water saturation and the max relative permeability to gas, which have a direct impact on the relative permeability to gas and on the capacity, as shown in the graph.

The only parameters that show no impact on the storage capacity are anisotropy ratio and porosity. Taking into account, that in this study and in the case of porosity's sensitivity, the GWC was modified to have the same reservoir size in all the cases; so, the analysis was more on the contribution of the trapping mechanisms and migration of CO_2 plume in the reservoir with change of porosity, to have a more reasonable comparison between the cases.

2. Injection strategy

Two analyses were discussed concerning the injection strategy, the constant injection rate and the ramp-up injection strategy.

The results have shown that in both analyses the cumulative stored CO_2 was the same, however the injectivity was affected. The same comparison will be done on the other parameters already investigated to compare their effect on the injectivity.

Figure 62 Injection duration for the different constant rates

The comparison of the difference between the well bottom hole pressure and the well block pressure is made at the year 2071:

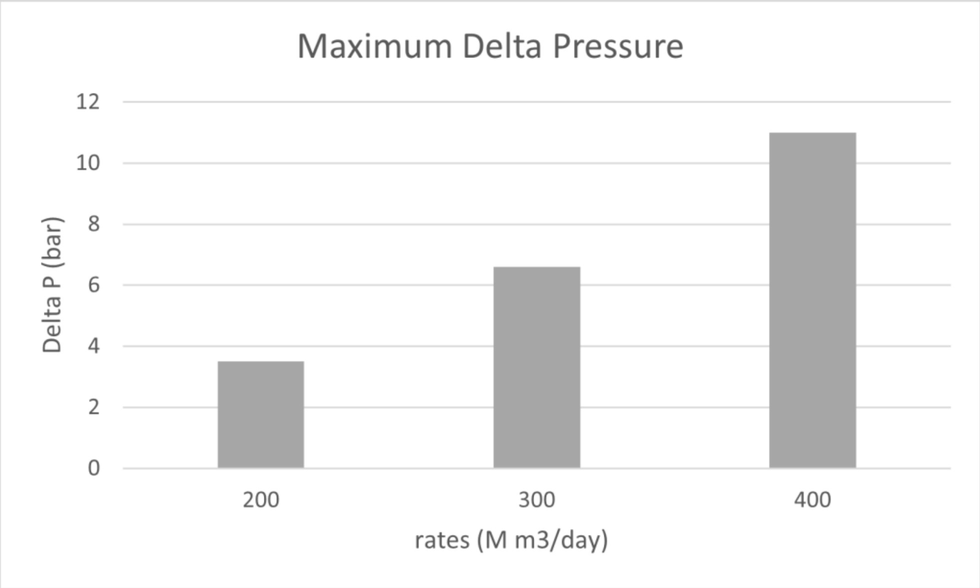

Figure 63 Delta Pressure for diff injection rates

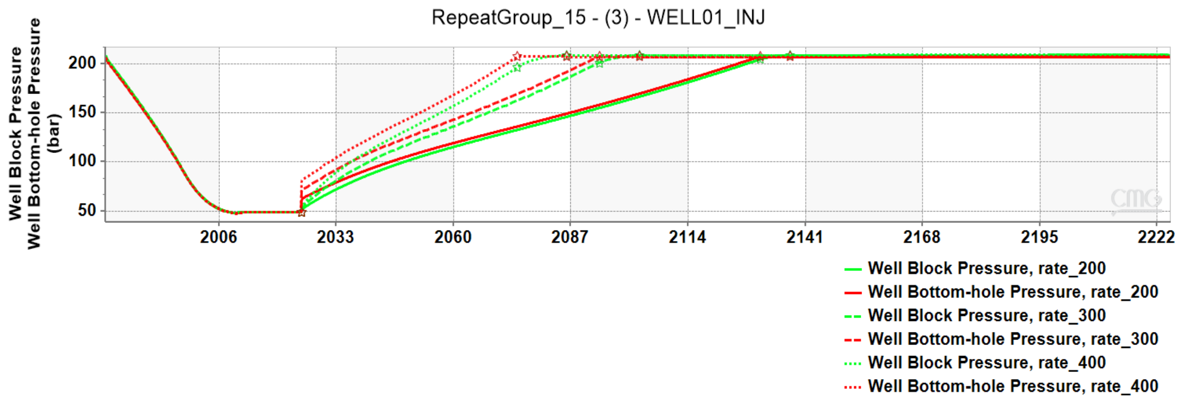

Figure 64 WBHP and Block Pressure profiles

Concerning the injection rates, the highest rate presents the shortest duration of injection which can be considered beneficial for achieving the desired storage amounts in a short period of time. As well as concerning the pressure drawdown where it increases with the increasing of rate since greater amount of CO_2 is being injected relative to the other cases therefore the block pressure increases near the wells.

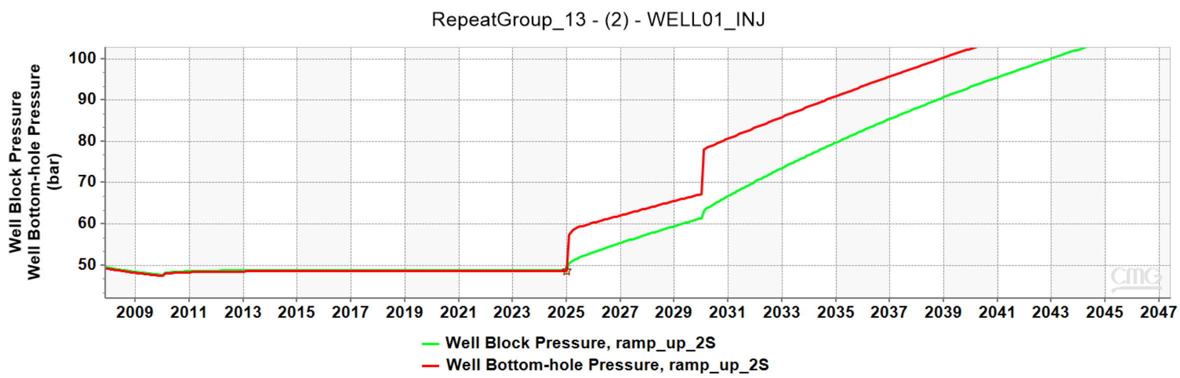

Figure 65 Maximun delta pressure (2 steps)

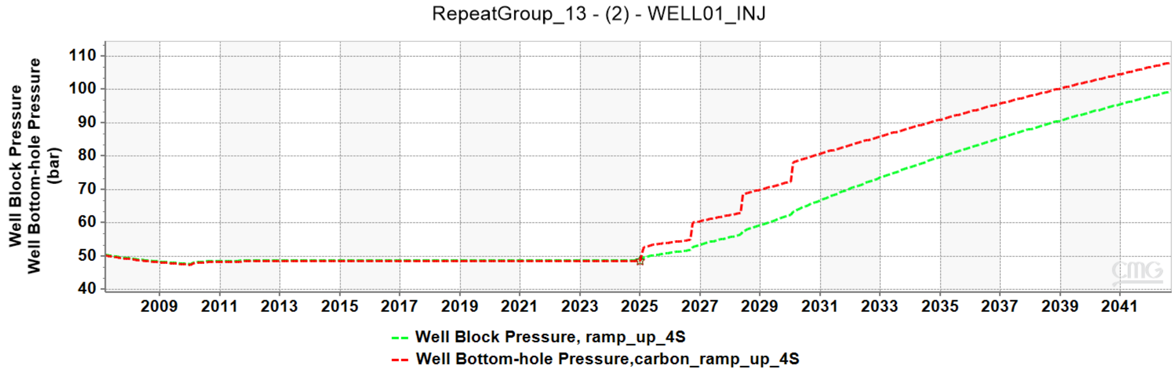

Figure 66 Maximum delta pressure (4 steps)

As seen on the graph, the maximum delta pressure increases gradually in the case of a ramp-up injection which helps in controlling the delta pressure applied to the well bottom hole. With increasing the number of steps, the maximum delta pressure increases more gradually under control. Moreover, there is no big difference between both cases other than the gradual increase of maximum pressure since geomechanical aspects were not considered in these simulations.

3. Trapping mechanisms

With the variation of the key parameters, an important variation related to the trapping mechanisms resulted in each sensitivity. In the following graph a summary of how each parameter affects the potential of different trapping mechanisms.

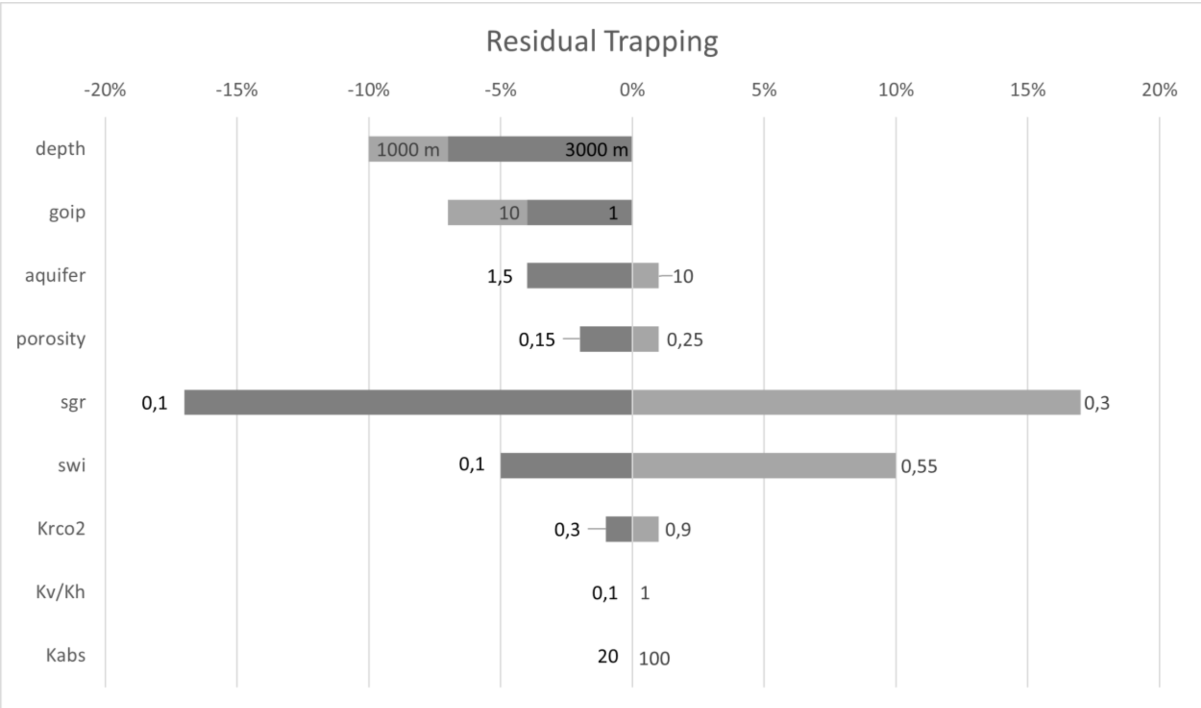

Figure 67 Residual trapping change with parameters

Concerning residual trapping, the parameter that affects it widely is the residual gas saturation since it is related directly to the mechanism of this trapping and in second place the irreducible water saturation since the immobile water present in the pores of the reservoir can play an important role in affecting the amount of CO_2 trapped in the pores.

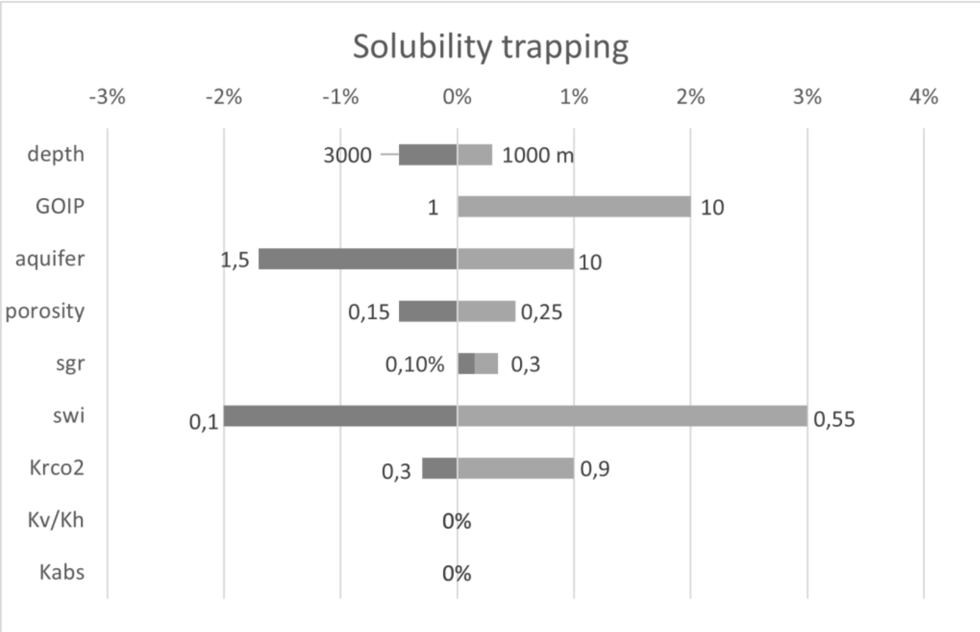

Figure 68 Solubility trapping change with parameters

The solubility trapping main variation is dominated by the irreducible water saturation which as discussed previously has a direct correlation with the amount of CO_2 dissolved in the reservoir since the injected gas has more water to be dissolved in in a case with high Swi. In addition, the surrounding aquifer size also shows an important effect on the solubility trapping due to water encroachment as investigated previously in the analysis part.

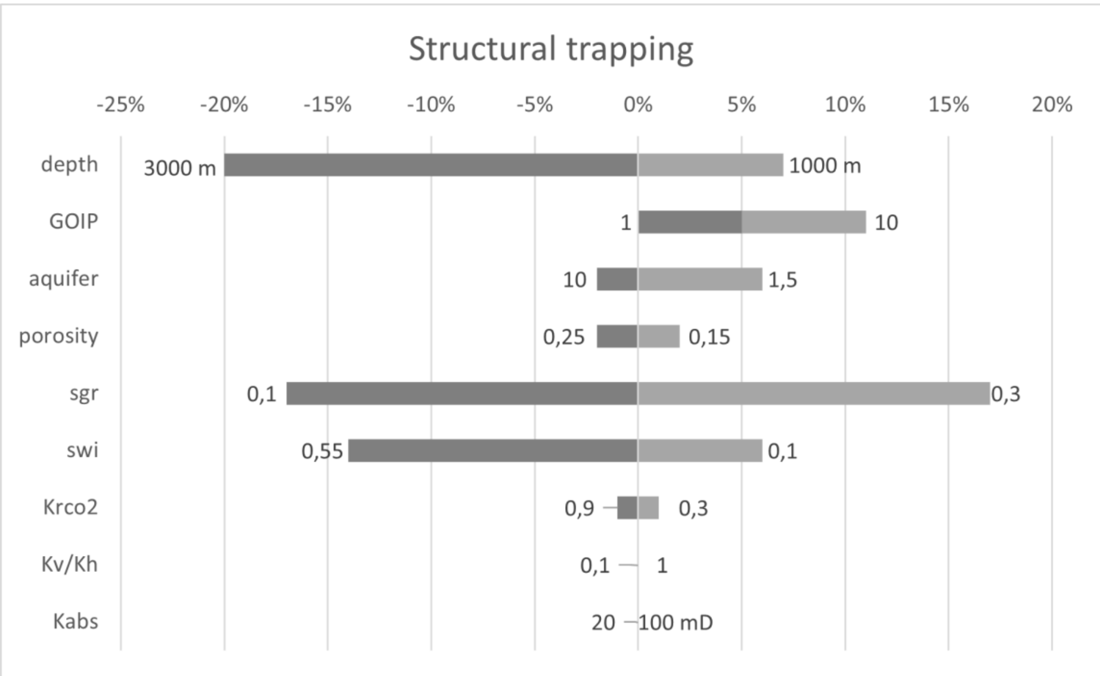

Figure 69 Structural Trapping change with parameters

First, it is important to notice that the structural trapping is the dominant mechanism in the different analyses performed. It is influenced by various parameters, mainly the reservoir depth as the CO_2 parameters (mainly viscosity and density) change with depth which may affect the free gas in the reservoir. Residual gas saturation and irreducible water saturation, both have an important impact on the contribution of the structural trapping of CO_2 since they affect mainly the residual and solubility trapping which can consequently be translated in a change in the structural trapping and moreover, the presence of the gas and water in the pores can affect the CO_2 migration and free amount in the reservoir as already discussed.

The mineral and ionic trapping was considered only in one case of the sensitivities which is the depth as already justified previously. The mineral trapping plays a very important role with the increase of depth due to temperature and pressure increase with depth. The following chart summarizes the increase in mineral and ionic trapping with depth.

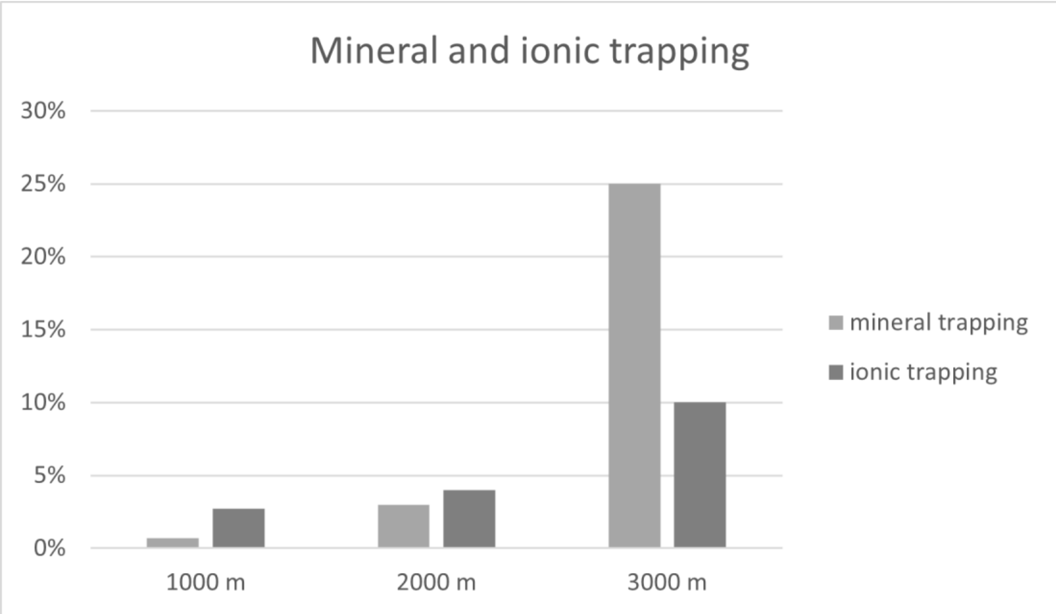

Figure 70 Mineral and ionic trapping (sensitivity: depth)

VII. Conclusion

This study provides a comprehensive analysis of the underground storage of CO_2 in depleted gas reservoirs by examining different key factors having impact on the storage capacity and injectivity, thus on the efficiency of the injection. Numerical simulations were conducted to highlight the different behavior of the reservoir and the different trapping mechanisms' contributions caused by different parameters.

From the storage capacity point of view, key findings from the sensitivity analysis reveal that overall, the structural trapping, indicated by the free gas amount, is the dominant mechanism in all cases. The highest influence on the storage capacity was the GOIP, in other words the reservoir size and the least influence was the anisotropy ratio presenting, as expected, no impact in the CO_2 amount. Reservoir depth and aquifer size have both a crucial effect on the storage capacity of CO_2 mainly by influencing specific trapping mechanisms, since the aquifer size has a direct influence on the dissolution trapping and the reservoir depth affects the CO_2 properties thus different trapping mechanisms contributions. Porosity affects the trapping mechanisms due to the change in the pore spaces. Residual gas saturation presents a direct and crucial influence on the residual trapping mechanism as well as on the structural trapping mechanism. The amount of irreducible water saturation is playing a key factor in changing the solubility trapping potential as well as the residual trapping one. The effective permeability to CO2 has shown an impact on the pressure dissipation in the reservoir

From the injection strategy point of view, higher rates present a faster injection as well as higher injectivity, however, pressure management is crucial in these cases to assure the integrity of the reservoir. Moreover, some ramp-up injection strategies were simulated. The number of steps doesn't have a direct influence on the storage capacity but on the control of the delta-pressure applied to the well bottom-hole.

BIBLIOGRAPHY

[1] NASA. (n.d.). *Effects - NASA science*. NASA. https://science.nasa.gov/climate-change/effects/

[2] Lindsey, R. (2022, June 17). *Climate change: Annual Greenhouse Gas Index*. NOAA Climate.gov. https://www.climate.gov/news-features/understanding-climate/climate-change-annual-greenhouse-gas-index

[3] *Why is carbon dioxide harmful to the environment?* Blog - why is CO2 bad for the planet? (n.d.). https://www.moretrees.eco/blogs/why-is-carbon-dioxide-harmful-to-the-environment

[4] IEA (2020), Global energy-related CO2 emissions by sector, IEA, Paris https://www.iea.org/data-and-statistics/charts/global-energy-related-co2-emissions-by-sector, License: CC BY 4.0

[5] *The Paris Agreement*. Unfccc.int. (n.d.). https://unfccc.int/process-and-meetings/the-paris-agreement

[6] United Nations. (n.d.). *The Paris Agreement*. United Nations. https://www.un.org/en/climatechange/paris-agreement

[7] 'The European Green Deal - COMMUNICATION FROM THE COMMISSION TO THE EUROPEAN PARLIAMENT, THE EUROPEAN COUNCIL, THE COUNCIL, THE EUROPEAN ECONOMIC AND SOCIAL COMMITTEE AND THE COMMITTEE OF THE REGIONS', European Commission, Brussels, Dec. 2019.

[8] Iea. (n.d.). *Net zero emissions by 2050 scenario (NZE) – global energy and climate model – analysis*. IEA. https://www.iea.org/reports/global-energy-and-climate-model/net-zero-emissions-by-2050-scenario-nze

[9] IEA (2020), CCUS in Clean Energy Transitions, IEA, Paris https://www.iea.org/reports/ccus-in-clean-energy-transitions, Licence: CC BY 4.0

[10] IEA (2021), Net Zero by 2050, IEA, Paris https://www.iea.org/reports/net-zero-by-2050, Licence: CC BY 4.0

[11] IPCC, 2005: IPCC Special Report on Carbon Dioxide Capture and Storage. Prepared by Working Group III of the Intergovernmental Panel on Climate Change [Metz, B., O. Davidson, H. C. de Coninck, M. Loos, and L. A. Meyer (eds.)]. Cambridge University Press, Cambridge, United Kingdom and New York, NY, USA, 442 pp.

[12] Global CCS institute. (2023b). (rep.). *SCALING UP THROUGH 2030*. Retrieved 2024, from https://www.globalccsinstitute.com/wp-content/uploads/2024/01/Global-Status-of-CCS-Report-1.pdf.

[13] Ajayi, T., Gomes, J.S. & Bera, A. A review of CO2 storage in geological formations emphasizing modeling, monitoring and capacity estimation approaches. Pet. Sci. 16, 1028–1063 (2019). https://doi.org/10.1007/s12182-019-0340-8

[14] Bentham, M., & Kirby, G.A. (2005). CO2 Storage in Saline Aquifers. Oil & Gas Science and Technology-revue De L Institut Francais Du Petrole, 60, 559-567.

[15] Muhammad Ali, Nilesh Kumar Jha, Nilanjan Pal, Alireza Keshavarz, Hussein Hoteit, Mohammad Sarmadivaleh, Recent advances in carbon dioxide geological storage, experimental procedures, influencing parameters, and future outlook, Earth-Science Reviews, Volume 225, 2022, 103895

[16] Samuel Krevor, Martin J. Blunt, Sally M. Benson, Christopher H. Pentland, Catriona Reynolds, Ali Al-Menhali, Ben Niu, Capillary trapping for geologic carbon dioxide storage – From pore scale physics to field scale implications, International Journal of Greenhouse Gas Control, Volume 40, 2015, Pages 221-237, ISSN 1750-5836, https://doi.org/10.1016/j.ijggc.2015.04.006.

[17] Pan, Z., Ye, J., Zhou, F., Tan, Y., Connell, L. D., & Fan, J. (2018). CO2 storage in coal to enhance coalbed methane recovery: a review of field experiments in China. International Geology Review, 60(5–6), 754–776. https://doi.org/10.1080/00206814.2017.1373607

[18] Spagnoli, F., Dinelli, E., Giordano, P., Marcaccio, M., Zaffagnini, F., & Frascari, F. (2014). Sedimentological, biogeochemical and mineralogical facies of northern and central western Adriatic Sea. *Journal of Marine Systems*, *139*, 183–203. https://doi.org/10.1016/j.jmarsys.2014.05.021

[19] Bachu, Stefan & Shaw, J.. (2003). Evaluation of the CO Sequestration Capacity in Alberta's Oil and Gas Reservoirs at Depletion and the Effect of Underlying Aquifers. Journal of Canadian Petroleum Technology - J CAN PETROL TECHNOL. 42. 10.2118/03-09-02.

[20] Shi-xin Dai, Yan-jiao Dong, Feng Wang, Zhen-han Xing, Pan Hu, Fu Yang, 2022. A sensitivity analysis of factors affecting in geologic CO2 storage in the Ordos Basin and its contribution to carbon neutrality, China Geology, 5, 359-371. doi: 10.31035/cg2022019.

[21] Tsar, Mitchel & Ghasemiziarhani, Mohsen & Ofori, Kofi & Bahrami, Nick & Iglauer, S. (2013). The Effect of Well Orientation (Vertical vs. Horizontal) on CO_2 Sequestration in a Water Saturated Formation-saline Aquifer in Western Australia - (SPE-164935). 10.3997/2214-4609.20130502.

[22] Stefan Bachu, CO2 storage in geological media: Role, means, status and barriers to deployment, Progress in Energy and Combustion Science, Volume 34, Issue 2, 2008, Pages 254-273, ISSN 0360-1285, https://doi.org/10.1016/j.pecs.2007.10.001.

[23] Hughes, D. S. (2009). Carbon storage in depleted gas fields: Key challenges. Energy Procedia, 3007-3014.

[24] Dongxiao Zhang, Juan Song, Mechanisms for Geological Carbon Sequestration, Procedia IUTAM, Volume 10, 2014, Pages 319-327, ISSN 2210-9838, https://doi.org/10.1016/j.piutam.2014.01.027.

[25] Verma Y, Vishal V and Ranjith PG (2021) Sensitivity Analysis of Geomechanical Constraints in CO2 Storage to Screen Potential Sites in Deep Saline Aquifers. Front. Clim. 3:720959. doi: 10.3389/fclim.2021.720959

[26] Stefan Bachu, W.D. Gunter, E.H. Perkins, Aquifer disposal of CO2: Hydrodynamic and mineral trapping, Energy Conversion and Management, Volume 35, Issue 4, 1994, Pages 269 279, ISSN 0196-8904, https://doi.org/10.1016/0196-8904(94)90060-4.

[27] Shchipanov A, Kollbotn L, Encinas M, Fjelde I, Berenblyum R. Periodic CO2 Injection for Improved Storage Capacity and Pressure Management under Intermittent CO2 Supply. Energies. 2022; 15(2):566. https://doi.org/10.3390/en15020566

[28] Gonet, Kamil & Blicharski, Jacek & Rybicki, Czesław. (2015). The analysis of CO2 injection in depleted gas reservoirs during the sequestration process. AGH Drilling, Oil, Gas. 32. 185. 10.7494/drill.2015.32.1.185.

[29] Geothermal Reservoir Engineering, Malcolm Alister Grant , Paul F Bixley, Edition 2, Academic Press, 2011, ISBN 0123838819, 9780123838810

[30] Gundogan, Ozgur. “Geochemical modelling of CO2 storage.” (2011).

[31] Akai, T.; Saito, N.; Hiyama, M.; Okabe, H. Numerical Modelling on CO2 Storage Capacity in Depleted Gas Reservoirs. Energies 2021, 14, 3978. https://doi.org/ 10.3390/en14133978

[32] Ramharack, Richard M., "Impact of carbon dioxide sequestration in depleted gas-condensate reservoirs" (2010). Graduate Theses, Dissertations, and Problem Reports. 2136. https://researchrepository.wvu.edu/etd/2136

[33] Moodie, N.; Ampomah, W.; Jia, W.; McPherson, B. Relative Permeability: A Critical Parameter in Numerical Simulations of Multiphase Flow in Porous Media. Energies 2021, 14, 2370. https://doi.org/10.3390/ en14092370

[34] Samin Raziperchikolaee, Ashwin Pasumarti, The impact of the depth-dependence of in situ stresses on the effectiveness of stacked caprock reservoir systems for CO2 storage, Journal of Natural Gas Science and Engineering, Volume 79, 2020, 103361, ISSN 1875-5100, https://doi.org/10.1016/j.jngse.2020.103361.

[35] Heidarabad, R.G.; Shin, K. Carbon Capture and Storage in Depleted Oil and Gas Reservoirs: The Viewpoint of Wellbore Injectivity. Energies 2024, 17, 1201. https://doi.org/10.3390/en17051201

[36] Naum I. Gershenzon, Robert W. Ritzi, David F. Dominic, Edward Mehnert, Roland T. Okwen, Capillary trapping of CO2 in heterogeneous reservoirs during the injection period, International Journal of Greenhouse Gas Control, Volume 59, 2017, Pages 13-23, ISSN 1750 5836, https://doi.org/10.1016/j.ijggc.2017.02.002.

[37] Lindsey, R. (2024, April 9). *Climate change: Atmospheric carbon dioxide*. NOAA Climate.gov. https://www.climate.gov/news-features/understanding-climate/climate-change-atmospheric-carbon-dioxide

[38] Wei, B., Wang, B., Li, X., Aishan, M., Ju, Y. CO2 storage in depleted oil and gas reservoirs: A review. Advances in Geo-Energy Research, 2023, 9(2): 76-93. https://doi.org/10.46690/ager.2023.08.02

[39] Chawarwan Khan, Robert Amin, Gary Madden, Carbon dioxide injection for enhanced gas recovery and storage (reservoir simulation), Egyptian Journal of Petroleum, Volume 22, Issue 2, 2013, Pages 225-240, ISSN 1110-0621, https://doi.org/10.1016/j.ejpe.2013.06.002.

[40] Chi-Chung Tseng, Bieng-Zih Hsieh, Shin-Tai Hu, Zsay-Shing Lin, Analytical approach for estimating CO2 storage capacity of produced gas reservoirs with or without a water drive, International Journal of Greenhouse Gas Control, Volume 9, 2012, Pages 254-261, ISSN 1750-5836, https://doi.org/10.1016/j.ijggc.2012.04.002.

[41] Bachu, S., and J. Shaw. "Evaluation of the CO2 Sequestration Capacity in Alberta's Oil and Gas Reservoirs at Depletion and the Effect of Underlying Aquifers." J Can Pet Technol 42 (2003): No Pagination Specified. doi: https://doi.org/10.2118/03-09-02

[42] Wang X, Zhang Q and Wan Y (2024), A twophase, multi-component model for efficient CO2 storage and enhanced gas recovery in low permeability reservoirs. Front. Energy Res. 12:1373851. doi: 10.3389/fenrg.2024.1373851

[43] Nicolas C.M. Marty, Francis Claret, Arnault Lassin, Joachim Tremosa, Philippe Blanc, Benoit Madé, Eric Giffaut, Benoit Cochepin, Christophe Tournassat, A database of dissolution and precipitation rates for clay-rocks minerals, Applied Geochemistry, Volume 55, 2015.

[44] W.E Kline, H.S Fogler, Dissolution kinetics: Catalysis by salts, Journal of Colloid and Interface Science, Volume 82, Issue 1, 1981, Pages 103-115, ISSN 0021-9797, https://doi.org/10.1016/0021-9797(81)90128-4.

[45] Raza, Arshad & Gholami, Raoof & Rezaee, Reza & Rasouli, Vamegh & Bhatti, Amanat & Bing, Chua. (2018). Suitability of depleted gas reservoirs for geological CO2 storage: A simulation study. Greenhouse Gases: Science and Technology. 8. 10.1002/ghg.1802.

[46] Allen, Rebecca & Nilsen, Halvor & Andersen, Odd & Lie, Knut-Andreas. (2017). On obtaining optimal well rates and placement for CO2 storage. Computational Geosciences. 21. 10.1007/s10596-017-9631-6.

[47] Chu, B.; Feng, G.; Zhang, Y.; Qi, S.; Li, P.; Huang, T. Residual Saturation Effects on CO2 Migration and Caprock Sealing: A Study of Permeability and Capillary Pressure Models. Water 2023, 15, 3316. https://doi.org/10.3390/w15183316

[48] Arshad Raza, Raoof Gholami, Reza Rezaee, Chua Han Bing, Ramasamy Nagarajan, Mohamed Ali Hamid, CO2 storage in depleted gas reservoirs: A study on the effect of residual gas saturation, Petroleum, Volume 4, Issue 1, 2018, Pages 95-107, ISSN 2405-6561, https://doi.org/10.1016/j.petlm.2017.05.005.

[49] Oldenburg, Curtis & Doughty, Christine. (2010). Injection, Flow, and Mixing of CO_2 in Porous Media with Residual Gas. Transport in Porous Media. 90. 201-218. 10.1007/s11242-010-9645-1.

[50] Rasool, M.H.; Ahmad, M.; Ayoub, M. Selecting Geological Formations for CO_2 Storage: A Comparative Rating System. Sustainability 2023, 15, 6599. https://doi.org/10.3390/su15086599